

5.1 INTRODUCTION	2
5.1.1 <i>Balanced Composite Curves</i>	3
5.1.2 <i>Estimating Operating, Capital and Annualized Total Costs</i>	11
5.2 HEAT-EXCHANGE AREA AND CAPITAL COST TARGETS FOR 1-1 EXCHANGERS.....	14
5.2.1 <i>Heat-Exchange Area with a Constant Overall Heat-Transfer Coefficient</i>	14
5.2.2 <i>Heat-Exchange Area with Individual Film Heat-Transfer Coefficients</i>	19
5.2.3 <i>Capital Cost Targets</i>	27
5.3 HEAT-EXCHANGE AREA AND CAPITAL COST TARGETS FOR 1-2 EXCHANGERS.....	31
5.3.1 <i>Area Target for a Network of Single 1-2 Exchangers</i>	33
5.3.2 <i>Area Target for a Network with 1-2 Shells in Series</i>	37
5.3.3 <i>Predicting the Total Number of Shells and Capital Cost</i>	47
5.4 SUPERTARGETING: OPTIMIZING THE MINIMUM APPROACH TEMPERATURE.....	54
5.5 SUMMARY.....	58
NOMENCLATURE	60
REFERENCES	63

Chapter 5: Advanced Targeting: Area Costs, Capital Costs and DT_{\min} Optimization

5.1 Introduction

Previous chapters concentrated on developing a maximum-energy-recovery (MER) network by first identifying minimum utility targets and then generating a heat-exchanger network to meet those targets. However, we did not consider the economic feasibility of this network. This chapter introduces several powerful concepts of heat integration that extend the use of composite curves beyond utility targeting and network design. In fact, the composite curves, developed in Chapter 2, contain enough information to estimate the total cost of a heat-exchange network.

First, this chapter develops a technique for estimating the heat-exchange area for a simple network consisting of one-shell-pass and one-tube-pass (1-1) exchangers (Section 5.2). Then, it turns to the more complex task of targeting the heat-exchange area, number of shells and capital cost for a network of one-shell-pass and two-tube-pass (1-2) exchangers (Section 5.3). The chapter applies the targets for heat-exchange area and number of shells, in combination with heat-exchanger cost correlations, to optimize the minimum approach temperature, ΔT_{\min} , of a heat-exchanger network prior to detailed design (Example 5.4).

The advantages of apply these techniques include (Smith, 1995):

- Evaluating alternative designs for the reactor and separation sections of a manufacturing process to minimize costs.

- Studying the implications of a variety of utility options (i.e., steam levels, furnaces and gas turbines) on heat-exchanger network costs.
- Optimizing the approach temperature, ΔT_{\min} , with respect to the total cost (Section 5.4).

Finally, Section 5.5 explores software applications for evaluating the heat-exchange area, capital cost and total cost of a heat-exchanger network as well as ΔT_{\min} optimization.

5.1.1 Balanced Composite Curves

The balanced composite curve is a modification of the hot and cold composite curves *to include heating and cooling utilities*. In this case, the minimum heating- and cooling-utility duties, identified on the balanced composite curve become zero.

Returning to Example 2.1, Table 5.1 lists the hot and cold streams of the original example. In addition, the table includes a hot-utility stream representing steam (1505 kW) condensing from 210 C to 209 °C, and a cold-utility stream representing cooling water (1375 kW) with supply and target temperatures of 30 and 40 °C, respectively. We assume a temperature drop of 1 °C for the constant-temperature heating utility (see Section 2.5.2). This enables us to calculate an equivalent capacity flowrate for the heating steam by dividing the total heating duty by the assumed temperature drop.

Chapter 4 discusses utility selection and placement with respect to the grand composite curve.

Table 5.1. Balanced stream data for Example 2.1 including heating (H3) and cooling (C3) utility streams.

Stream	T^{supply}_i	T^{target}_i	$(MC_p)_i$	DH_i
i	(°C)	(°C)	(kW/°C)	(kW)
H1	185	55	20	2600
H2	135	75	40	2400
H3	210	209	1505	1505
C1	50	185	30	4050
C2	70	142	15	1080
C3	20	30	137.5	1375

Table 5.2 is a temperature-interval diagram (TID) for Example 2.1 through the balanced stream data of Table 5.1. Figure 5.1 is the balanced composite curve for Example 2.1 constructed from the composite hot and cold streams of Table 5.2. We find that the heating- and cooling-utility duties are zero from both the TID and balanced composite curves.

Table 5.2. Balanced TID for Example 2.1 including heating- and cooling-utility streams H3 and C3, respectively.

Shifted Temperature (°C)	Hot Streams			Heat Surplus (kW)	Cumulative Surplus (kW)	Cold Streams			Heat Deficit (kW)	Cumulative Deficit (kW)	Net Heat Surplus (kW)	Cascaded Surplus (kW)	Adjusted Surplus (kW)
	H1 20 kW/°C	H2 40 kW/°C	H3 1505 kW/°C			C1 30 kW/°C	C2 15 kW/°C	C3 137.5 kW/°C					
30					0					0		0	0
				0				↓	1375		-1375		
40					0			↓		1375		1375	1375
				0					0		0		
45	↑				0					1375		1375	1375
				300					0		300		
60					300			↓		1375		1075	1075
				100					150		-50		
65		↑			400					1525		1125	1125
				900					450		450		
80					1300			↓		1975		675	675
				2700					2025		675		
125					4000					4000		0	0
				540					1215		-675		
152					4540			↓		5215		675	675
				460					690		-230		
175					5000					5905		905	905
				0					600		-600		
195					5000			↓		6505		1505	1505
				0					0		0		
199					5000					6505		1505	1505
			↑		1505				0		1505		
200					6505					6505		0	0

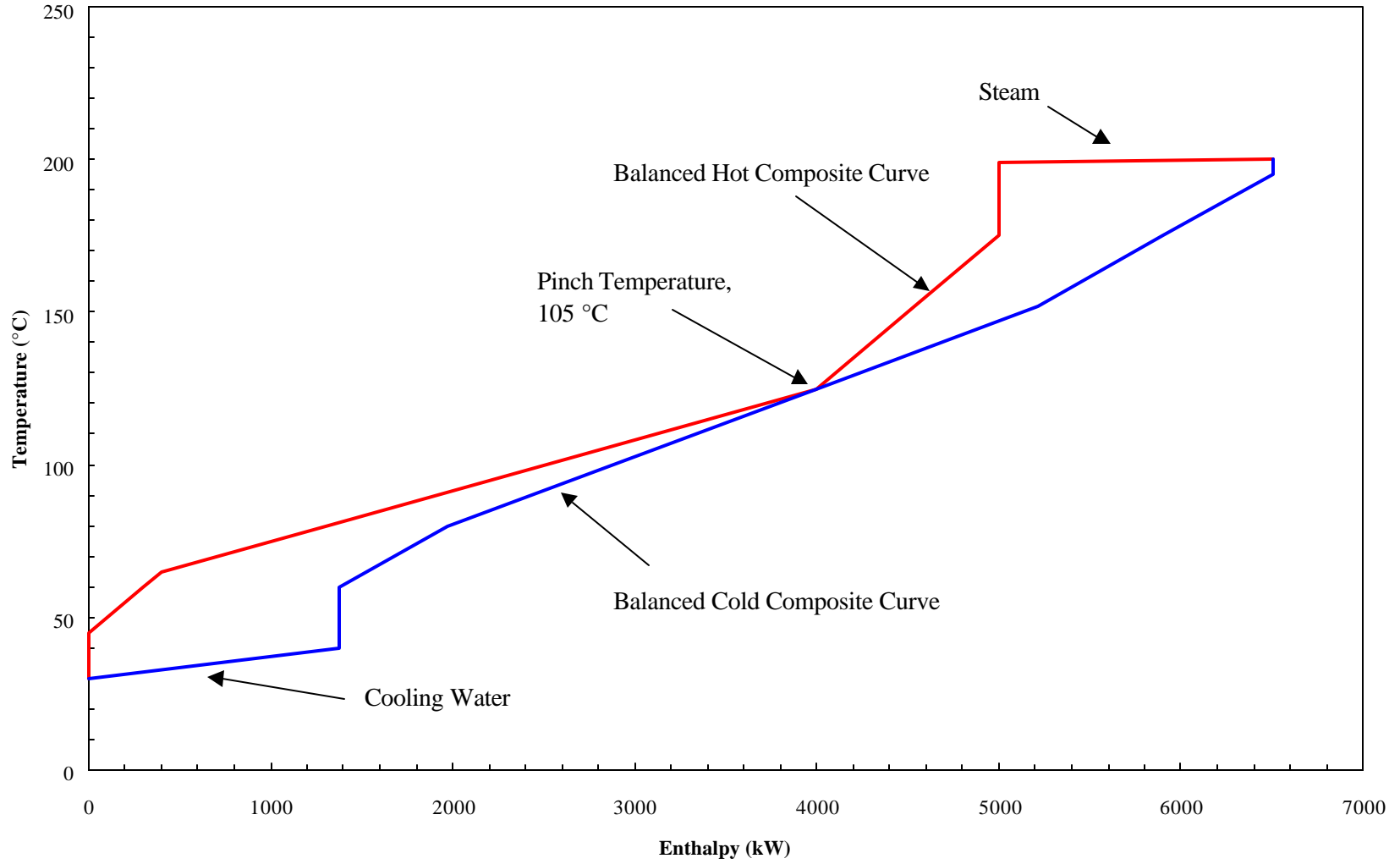


Figure 5.1. Balanced composite curves for Example 2.1. Temperatures shifted for a minimum approach temperature of 20 °C.

Figure 5.2 divides the balanced composite curve for Example 2.1 into seven vertical enthalpy intervals. In later sections, we will require the specific unshifted supply and target temperatures of the hot and cold composite curves defined by each enthalpy interval created in Figure 5.2. Note that for each enthalpy interval, at least two of these temperatures will correspond to the temperature-interval boundaries defined by the limiting process data. The other two are either determined graphically or rigorously calculated from the capacity flowrates and enthalpy change in each interval. Figure 5.3 illustrates these temperatures and the position of each stream with respect to the enthalpy intervals created in Figure 5.2. It shows the unshifted supply and target temperatures for the hot composite curve above enthalpy-interval boundaries, and those temperatures for the cold composite curve below interval boundaries. This figure also lists two temperatures for discontinuous enthalpy intervals (e.g., “50.00/30.00 °C” on the cold side identifies a discontinuity on the cold composite curve at the 3rd enthalpy-interval boundary).

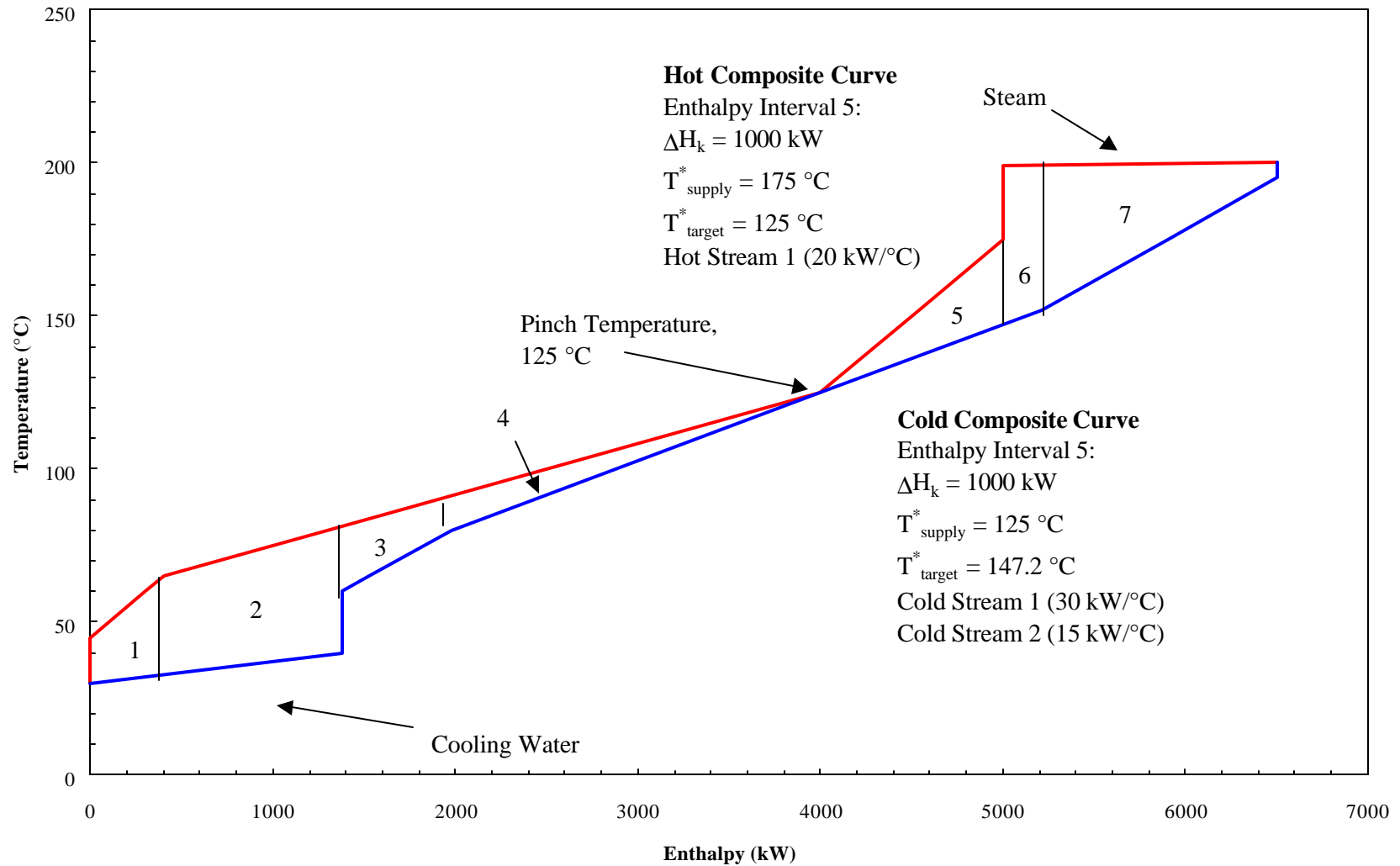


Figure 5.2. Balanced composite curves for Example 2.1 divided into vertical entalpy intervals. Temperatures shifted for a minimum approach temperature of $20 \text{ }^\circ\text{C}$.

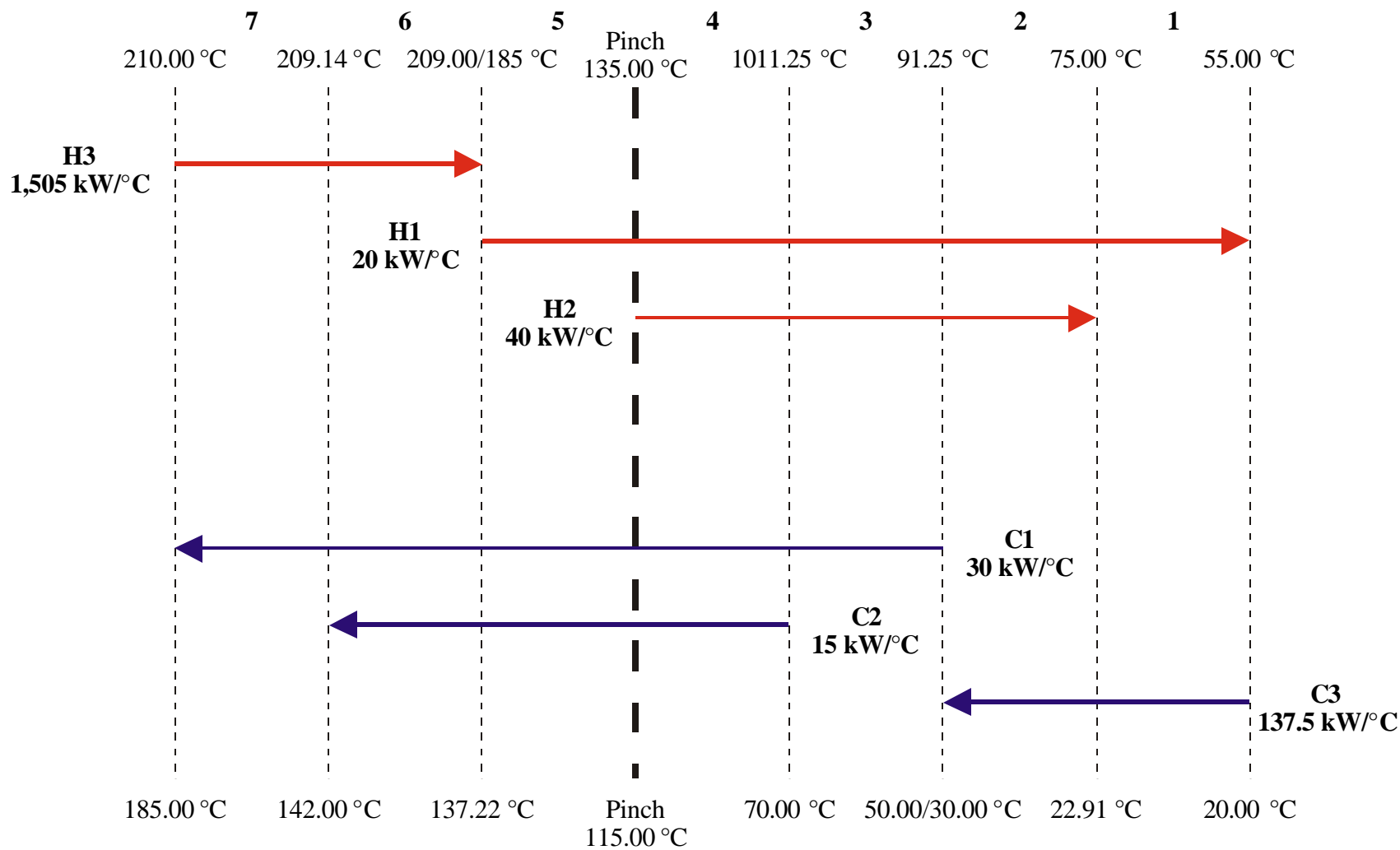


Figure 5.3. Vertical enthalpy intervals for Example 2.1 with the relative positions of hot and cold process and utility streams. Temperatures are unshifted. Hot-stream and cold-stream temperatures appear at the top and bottom of the diagram, respectively.

5.1.2 Estimating Operating, Capital and Annualized Total Costs

This section discusses how to determine operating, capital and annualized costs for a heat-exchanger network.

The operating cost of a heat-exchanger network includes the costs of heating and cooling utilities. Table 5.3 gives typical operating costs for some heating and cooling utilities. For Example 2.1, based on 8,000 hr/yr, we require 1375 kW of cooling from the cooling-water system (\$0.01/kWhr) and 1505 kW of heating from high-pressure steam (\$0.10/kWhr) to give an annual operating cost of 1,314,000 \$/yr (= \$110,000 + \$1,204,000).

Table 5.3. Typical costs for heating and cooling utilities in 1998 dollars (Douglas, 1988).

Utility	Cost
R-44 Refrigeration	\$0.034/(kW hr)
Cooling Water	\$0.04/1,000 gal
LP Steam	\$4.23/1,000 lb
HP Steam	\$5.62/1,000 lb
Electricity	\$0.05/(kW hr)
Fuel	\$4.98/10 ⁶ BTU

After estimating the total heat-exchange area, we will need correlations for the installed capital cost of heat exchangers. Heat-exchanger capital-cost correlations typically take the form of Equation 5.1:

$$\text{Exchanger Cost} = a + b(A_{\text{network}})^c \quad (5.1)$$

where the cost parameters a, b and c depend on specific materials of construction and types of exchanger. Here, the parameter, a, represents fixed costs. Table 5.4 lists the values of a, b and c for Equation 5.1 for a variety of exchangers.

Table 5.4. Heat-Exchanger cost-law parameters for Equation 5.1 for various types of exchangers in 1998 dollars (Douglas, 1988).

Exchanger Type	a (\$)	b (\$/m^{2c})	c
Carbon Steel (CS)	0	383.5	0.65
Stainless Steel (SS)	0	1438.1	0.65
Monel	0	1629.8	0.65

We can consider both the operating and capital costs of a heat-exchanger network by determining the total cost on an annualized basis. Equation 5.2 gives the total annualized cost (without interest) of a heat-exchanger network as a function of the operating and capital costs as:

$$(\text{Total Annualized Cost}) = (\text{Operation Cost}) + \frac{(\text{Capital Cost})}{t} \quad (5.2)$$

where t is the equipment lifetime in years.

From here, we turn to composite curves to estimate the heat-exchange area and capital costs.

5.2 Heat-Exchange Area and Capital Cost Targets for 1-1 Exchangers

The capital cost of a heat-exchanger network is directly dependent on the total heat-exchange area. Therefore, an estimate of the required area for a heat-exchanger network is necessary for evaluating its economic feasibility. If we can determine the area without constructing a network, we can quickly evaluate the capital costs of several alternative flowsheets.

As an introduction to area and capital-cost targeting for more complex industrial applications, this section presents a method for targeting the total area and capital cost for a network comprised of one-shell-pass and one-tube-pass (1-1) exchangers. We discuss heat-exchange area targeting for the simple case with a constant overall heat-transfer coefficient, and for the more complex case with individual film heat-transfer coefficients for hot and cold streams.

5.2.1 Heat-Exchange Area with a Constant Overall Heat-Transfer Coefficient

Using the balanced composite curve, we can evaluate the heat-exchange area of a process without constructing a network. Figure 5.2 illustrates the balanced composite curve for Example 2.1. This figure divides the problem into vertical enthalpy intervals. It allows us to evaluate heat-exchange matches between hot and cold streams existing in each vertical enthalpy interval. In particular, Figure 5.2 lists details for the fifth enthalpy interval, including the

enthalpy change, supply and target temperatures for hot and cold composite curves as well as the streams that exist in enthalpy interval k.

For simplicity, we first assume a constant overall heat-transfer coefficient, U. Later, we consider individual film heat-transfer coefficients. With a constant overall heat-transfer coefficient, the heat-exchange area in an enthalpy interval is:

$$A_{1-1,k} = \frac{\Delta H_k}{U \Delta T_{LM,k}} \quad (5.3)$$

where $A_{1-1,k}$, ΔH_k , $\Delta T_{LM,k}$ are the 1-1 heat-exchange area, enthalpy change and log-mean temperature difference (LMTD) for enthalpy interval k, respectively. The LMTD for an enthalpy interval is:

$$\Delta T_{LM,k} = \frac{(T_{HCC,k}^{supply} - T_{CCC,k}^{target}) - (T_{HCC,k}^{target} - T_{CCC,k}^{supply})}{\ln \left(\frac{T_{HCC,k}^{supply} - T_{CCC,k}^{target}}{T_{HCC,k}^{target} - T_{CCC,k}^{supply}} \right)} \quad (5.4)$$

where $T_{HCC,k}^{supply}$ and $T_{HCC,k}^{target}$ are the unshifted supply and target temperatures defined on the hot composite curve, and $T_{CCC,k}^{supply}$ and $T_{CCC,k}^{target}$ are the unshifted supply and target temperatures defined on the cold composite curve by enthalpy interval k.

The total 1-1 heat-exchange area, $A_{1-1, network}$, is the sum of Equation 5.3 over all enthalpy intervals:

$$A_{1-1, \text{network}} = \frac{1}{U} \sum_k \frac{\Delta H_k}{\Delta T_{LM,k}} \quad (5.5)$$

Returning to Example 2.1, we assume a constant overall heat-transfer coefficient of $0.1 \text{ kW}/(\text{°C}\cdot\text{m}^2)$. Figure 5.3 depicts hot and cold process and utility streams as well as the unshifted supply and target temperatures of hot and cold composite curves as defined by vertical enthalpy intervals. For example, Figure 5.4 shows hot and cold composite curves (HCC and CCC) in the fifth enthalpy interval created in Figures 5.2 and 5.3. Specifically, for the fifth enthalpy interval of Example 2.1, Equation 5.4 gives the log-mean temperature difference as:

$$\begin{aligned} \Delta T_{LM,5} &= \frac{(T_{HCC,5}^{\text{supply}} - T_{CCC,5}^{\text{target}}) - (T_{HCC,5}^{\text{target}} - T_{CCC,5}^{\text{supply}})}{\ln\left(\frac{T_{HCC,5}^{\text{supply}} - T_{CCC,5}^{\text{target}}}{T_{HCC,5}^{\text{target}} - T_{CCC,5}^{\text{supply}}}\right)} \\ &= \frac{(185 - 137.22) - (135 - 115)}{\ln\left(\frac{185 - 137.22}{135 - 115}\right)} \\ &= 31.90 \text{ °C} \end{aligned}$$

Table 5.5 lists the enthalpy change, the unshifted supply and target temperatures of hot and cold composite curves, the LMTD, and the resulting 1-1 heat-exchange area (Equation 5.3) for each enthalpy interval created on the balanced composite curve (Figures 5.3 and 5.4). Here, Equation 5.5 gives a total 1-1 heat-transfer area of 1882.3 m^2 .

Table 5.5. Data for determining the total 1-1 heat-exchange area for Example 2.1 through Equations 5.2 and 5.3, assuming a constant overall heat-transfer coefficient ($U = 0.1 \text{ kW}/(^{\circ}\text{C}\cdot\text{m}^2)$). Actual (unshifted) temperatures shown.

Enthalpy							
Interval	$\mathbf{DH_k}$	$\mathbf{T^{\text{supply}}_{\text{HCC},k}}$	$\mathbf{T^{\text{target}}_{\text{HCC},k}}$	$\mathbf{T^{\text{supply}}_{\text{CCC},k}$	$\mathbf{T^{\text{target}}_{\text{CCC},k}$	$\mathbf{DT_{LM},k}$	$\mathbf{A_{1-1},k}$
k	(kW)	(C)	(C)	(C)	(C)	(C)	(m ²)
1	400	75.00	55.00	20.00	22.91	42.98	93.07
2	975	91.25	75.00	22.91	30.00	56.55	172.42
3	600	101.25	91.25	50.00	70.00	36.02	166.58
4	2025	135.00	101.25	70.00	115.00	25.21	803.32
5	1000	185.00	135.00	115.00	137.22	31.90	313.50
6	215	209.14	209.00	137.22	142.00	69.43	30.96
7	1290	210.00	209.14	142.00	185.00	42.66	302.41
Total	6505						1882.26

The principal difficulty in applying Equations 5.2 through 5.4 to industrial heat-integration problems is that the overall heat-transfer coefficient, U , is not necessarily constant. We must account for a variety of heat-exchange matches (e.g., process stream to process stream versus process stream to utility stream) that may be necessary to meet the minimum heating- and cooling-utility targets. The following section presents an effective method for considering individual film heat-transfer coefficients for all process and utility streams.

5.2.2 Heat-Exchange Area with Individual Film Heat-Transfer Coefficients

We now return to the fifth enthalpy interval depicted in Figure 5.4 and consider individual matches between hot and cold streams. Figure 5.5 illustrates that for this enthalpy interval, we can design a heat-exchanger network that is guaranteed to require the minimum number of heat-exchange units ($S_k - 1$) (see Section 3.3.2). Here, S_k is the number of streams (hot, cold and utility streams) that exist within enthalpy interval k . Note that to reach the minimum number of units, we follow two simple guidelines. First, each hot (cold) stream in the heat-exchange unit must enter and exit the unit at the shifted supply and target temperatures of the hot (cold) composite curve, respectively. Second, the capacity-flowrate ratio for each hot to cold stream match, $\frac{(\dot{M}C_p)_{Hi}}{(\dot{M}C_p)_{Cj}}$, must equal the capacity-flowrate ratio of hot and cold composite curves within enthalpy interval k .

We determine the heat-exchange area for the subnetwork shown in Figure 5.5 by summing the area for each individual match within enthalpy interval 5.

$$A_k = \frac{1}{\Delta T_{LM,k}} \sum_i \sum_j \frac{Q_{Hi,Cj}}{U_{Hi,Cj}} \quad (5.6)$$

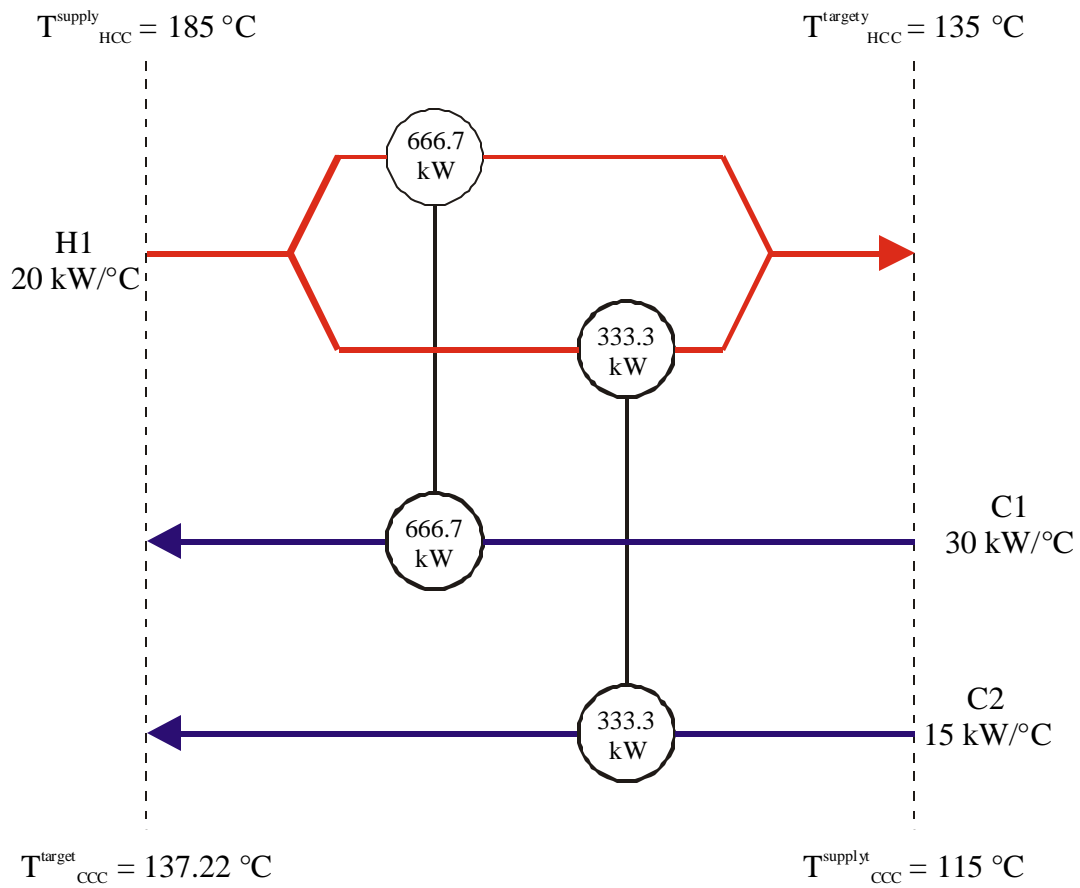


Figure 5.5. Heat-exchanger network for the fifth enthalpy interval of Example 2.1. Temperatures are unshifted.

where $\Delta T_{LM,k}$ is the LMTD defined by the supply and target temperatures of hot and cold composite curves for enthalpy interval k (Equation 5.4). $Q_{Hi,Cj}$ and $U_{Hi,Cj}$ are the heat duty and overall heat-transfer coefficient, respectively, for a match between hot stream i and cold stream j in enthalpy interval k . For each match between a hot stream i and a cold stream j within temperature interval k , we replace the overall heat-transfer coefficient, $U_{Hi,Cj}$, with the individual film heat-transfer coefficients for streams i and j . In this manner, we incorporate both wall and fouling resistances for both hot stream (h_{Hi}) and cold stream (h_{Cj}) for each heat-exchange unit in interval k .

$$A_{i-1,k} = \frac{1}{\Delta T_{LM,k}} \sum_i \sum_j Q_{Hi,Cj} \left(\frac{1}{h_{Hi}} + \frac{1}{h_{Cj}} \right) \quad (5.7)$$

Rearranging Equation 5.7 gives:

$$A_{i-1,k} = \frac{1}{\Delta T_{LM,k}} \sum_i \sum_j \left(\frac{Q_{Hi,Cj}}{h_{Hi}} + \frac{Q_{Hi,Cj}}{h_{Cj}} \right) \quad (5.8)$$

We can simplify Equation 5.7 with the following two substitutions to give Equation 5.11:

$$\sum_i \sum_j Q_{Hi,Cj} = \sum_i q_{Hi} \quad (5.9)$$

$$\sum_i \sum_j Q_{Hi,Cj} = \sum_j q_{Cj} \quad (5.10)$$

$$A_{1-1,k} = \frac{1}{\Delta T_{LM,k}} \left(\sum_i \frac{q_{Hi}}{h_{Hi}} + \sum_j \frac{q_{Cj}}{h_{Cj}} \right) \quad (5.11)$$

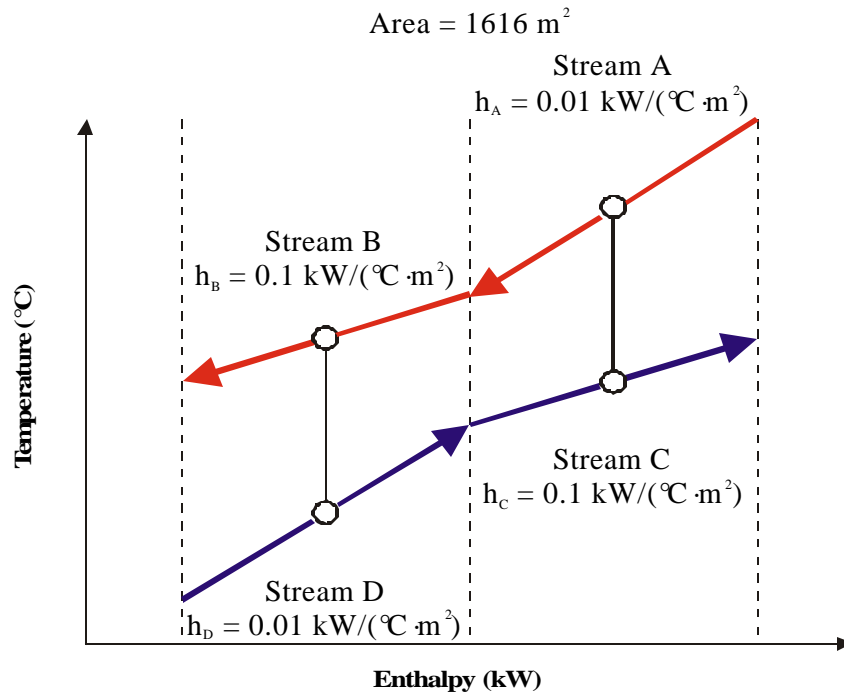
where q_{Hi} and q_{Cj} are the enthalpy changes of hot stream I and cold stream j in enthalpy interval k.

The total 1-1 heat-exchange area is the sum of Equation 5.11 over all enthalpy intervals:

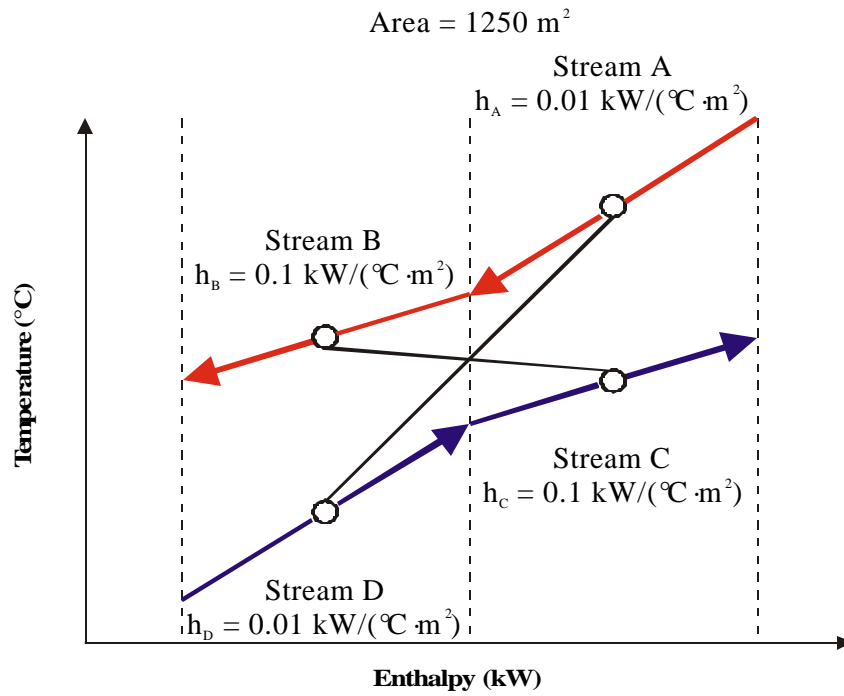
$$A_{1-1,\text{network}} = \sum_k \left[\frac{1}{\Delta T_{LM,k}} \left(\sum_i \frac{q_{Hi}}{h_{Hi}} + \sum_j \frac{q_{Cj}}{h_{Cj}} \right) \right] \quad (5.12)$$

In some cases, the heat-exchange area target calculated from Equation 5.12 can give area targets above that of the true minimum (Linnhoff and Ahmad, 1990). This results from our assumption that vertical heat transfer is most efficient. In cases where the film heat-transfer coefficients vary significantly, non-vertical heat transfer may be more efficient. In other words, we can reduce the total heat-transfer area (capital cost) of a network by matching hot streams with cold streams of similar film heat-transfer coefficients even if we cross enthalpy intervals. Figure 5.6 illustrates two adjacent enthalpy intervals and two alternative matching schemes.

Figure 5.6a shows the case where we make matches according to the assumption that vertical heat transfer is more efficient. In this case, we must match streams of significantly different film heat-transfer coefficients (0.1 to 0.01 kW/(°C·m²)). Figure 5.6a requires a heat-transfer area of 1616 m².



(a)



(b)

Figure 5.6. Two adjacent enthalpy intervals for a new example with significantly different film heat-transfer coefficients (Linnhoff and Ahmad, 1990)

On the other hand, when we allow non-vertical heat transfer, we match hot streams to cold streams with similar film heat-transfer coefficients and see a reduction in total heat-transfer area from 1616 to 1250 m². Here, we match stream A ($h_A = 0.01 \text{ kW}/(^{\circ}\text{C}\cdot\text{m}^2)$) with stream D ($h_D = 0.01 \text{ kW}/(^{\circ}\text{C}\cdot\text{m}^2)$), and stream B ($h_B = 0.1 \text{ kW}/(^{\circ}\text{C}\cdot\text{m}^2)$) with stream C ($h_C = 0.1 \text{ kW}/(^{\circ}\text{C}\cdot\text{m}^2)$).

Additionally, if the film heat-transfer coefficients vary by less than an order of magnitude, the error caused by the vertical heat-transfer assumption is less than 10 percent. Even so, the area prediction is useful for estimating the capital cost of a heat-exchanger network without specific knowledge of the network structure. The true minimum heat-exchange area can be determined using mathematical optimization (Saboo, et al., 1986).

Returning to Example 2.1, Table 5.6 lists the balanced stream data and individual film heat-transfer coefficients for each process and utility stream. Table 5.7 duplicates the unshifted supply and target temperatures of hot and cold composite curves as well as the log-mean temperature difference defined by vertical enthalpy intervals. The table also lists the individual enthalpies transferred from each hot stream and to each cold stream in each vertical enthalpy interval. The last column lists the 1-1 heat-exchange area required in each vertical enthalpy interval calculated through Equation 5.11. When considering individual film heat-transfer coefficients for Example 2.1, we use Equation 5.12 to estimate a minimum 1-1 heat-exchange area of 1732.6 m².

Table 5.6. Balanced stream data for Example 2.1 including individual film heat-transfer coefficients for each process and utility stream.

Stream	T^{supply}_I	T^{target}_I	$(MC_p)_I$	Duty	$h_{\text{film},i}$	Duty
i	(°C)	(°C)	(kW/°C)	(kW)	(kW/°C·m²)	(kW)
H1	185	55	20	2600	0.2	2600
H2	135	75	40	2400	0.2	2400
H3	210	209	1505	1505	0.4	1505
C1	50	185	30	4050	0.2	4050
C2	70	142	15	1080	0.2	1080
C3	20	30	137.5	1375	0.4	1375

Table 5.7. Data for determining the total 1-1 heat-transfer area for Example 2.1 through Equation 5.11 with individual film heat-transfer coefficients for each process and utility stream. Actual (unshifted) temperatures shown.

Enthalpy Interval k	Streams Present	$T^{\text{supply}}_{\text{HCC},k}$ (°C)	$T^{\text{target}}_{\text{HCC},k}$ (°C)	$T^{\text{supply}}_{\text{CCC},k}$ (°C)	$T^{\text{target}}_{\text{CCC},k}$ (°C)	$DT_{\text{lm},k}$ (°C)	Q_{H1} (kW)	Q_{H2} (kW)	Q_{H3} (kW)	Q_{C1} (kW)	Q_{C2} (kW)	Q_{C3} (kW)	$A_{1-1,k}$ (m ²)
1	H1,C3	75.00	55.00	20.00	22.91	42.98	400.00	0.00	0.00	0.00	0.00	400.00	69.80
2	H1,H2,C3	91.25	75.00	22.91	30.00	56.55	325.00	650.00	0.00	0.00	0.00	975.00	129.32
3	H1,H2,C1	101.25	91.25	50.00	70.00	36.02	200.00	400.00	0.00	600.00	0.00	0.00	166.58
4	H1,H2,C1,C2	135.00	101.25	70.00	115.00	25.21	675.00	1350.00	0.00	1350.00	675.00	0.00	803.32
5	H1,C1,C2	185.00	135.00	115.00	137.22	31.90	1000.00	0.00	0.00	666.67	333.33	0.00	313.50
6	H3,C1,C2	209.14	209.00	137.22	142.00	69.43	0.00	0.00	215.00	143.33	71.67	0.00	23.22
7	H3,C1	210.00	209.14	142.00	185.00	42.66	0.00	0.00	1290.00	1290.00	0.00	0.00	226.81
Total							2600.00	2400.00	1505.00	4050.00	1080.00	1375.00	1732.54

5.2.3 Capital Cost Targets

This section uses the 1-1 heat-exchange area target of the previous section to predict the installed capital cost of a heat-exchanger network prior to detailed design. We discussed a common correlation for the installed capital cost of a heat exchanger in Section 5.1.2 and now extend it to predict the installed capital cost of a network of exchangers based on the total 1-1 heat-exchange area prediction for that network.

A useful capital cost target is that for a network of 1-1 exchangers (i.e., single-shell pass and single-tube pass). An important extension of this technique is to evaluate the effect of more complex heat-exchanger units on area and capital cost targets.

To predict the installed capital cost of an entire network, we assume that the total heat-exchange area of a network is distributed equally across all of its units. In other words, all of the units have the same area. Recall that we determined the number of units, N_{units} , above and below the pinch (see Section 3.3.2):

$$N_{\text{units}} = (N_{\text{H}} + N_{\text{C}} + N_{\text{HU}})_{\text{above the pinch}} + (N_{\text{H}} + N_{\text{C}} + N_{\text{CU}})_{\text{below the pinch}} - 2 \quad (3.3)$$

We modify correlations of the form shown in Equation 5.1 to give the total installed capital cost of an entire network as a function of the number of units N_{units} and the total 1-1 heat-exchange area:

$$\text{Capital Cost} = N_{\text{units}} \left[a + b \left(\frac{A_{1-1, \text{network}}}{N_{\text{units}}} \right)^c \right] \quad (5.13)$$

Equation 5.13 gives installed network cost for a network of 1-1 exchangers.

In Section 3.3.2, we determined the minimum number of units for Example 2.1 from Equation 3.3:

$$\begin{aligned} N_{\text{units}} &= [N_{\text{H}} + N_{\text{C}} + N_{\text{HU}}]_{\text{Above the Pinch}} + [N_{\text{H}} + N_{\text{C}} + N_{\text{CU}}]_{\text{Below the Pinch}} - 2 \\ &= 4 + 5 - 2 \\ &= 7 \end{aligned}$$

Substituting the heat-exchange area for Example 2.1, determined in Table 5.5, into Equation 5.13 gives:

$$\begin{aligned} \text{Network Cost} &= N_{\text{units}} \left[a + b \left(\frac{A_{\text{network}}}{N_{\text{units}}} \right)^c \right] \\ &= (7) \left[0 + (3,000 \$/\text{m}^{1.5}) \left(\frac{1732.6 \text{ m}^2}{7} \right)^{0.75} \right] \\ &= \$1,310,000 \end{aligned}$$

For Example 2.1, a good estimate of the installed network cost for a system of 1-1 exchangers, heaters and coolers is \$1,310,000. We find the total annualized cost without interest from Equation 5.2:

$$\begin{aligned}(\text{Total Annualized Cost}) &= (\text{Operation Cost}) + \frac{(\text{Capital Cost})}{t} \\ &= \$1,314,000/\text{yr} + \frac{\$1,310,000}{5 \text{ yr}} \\ &= \$1,576,000/\text{yr}\end{aligned}$$

Figure 5.7 summarizes this method for estimating the heat-exchange area and installed cost for a network of 1-1 exchangers.

To be of industrial significance, we must be able to estimate capital costs for systems that require more complex heat exchangers (e.g., 1-shell-pass and 2-tube-pass exchangers). We shall discuss the latter aspects in Section 5.3.

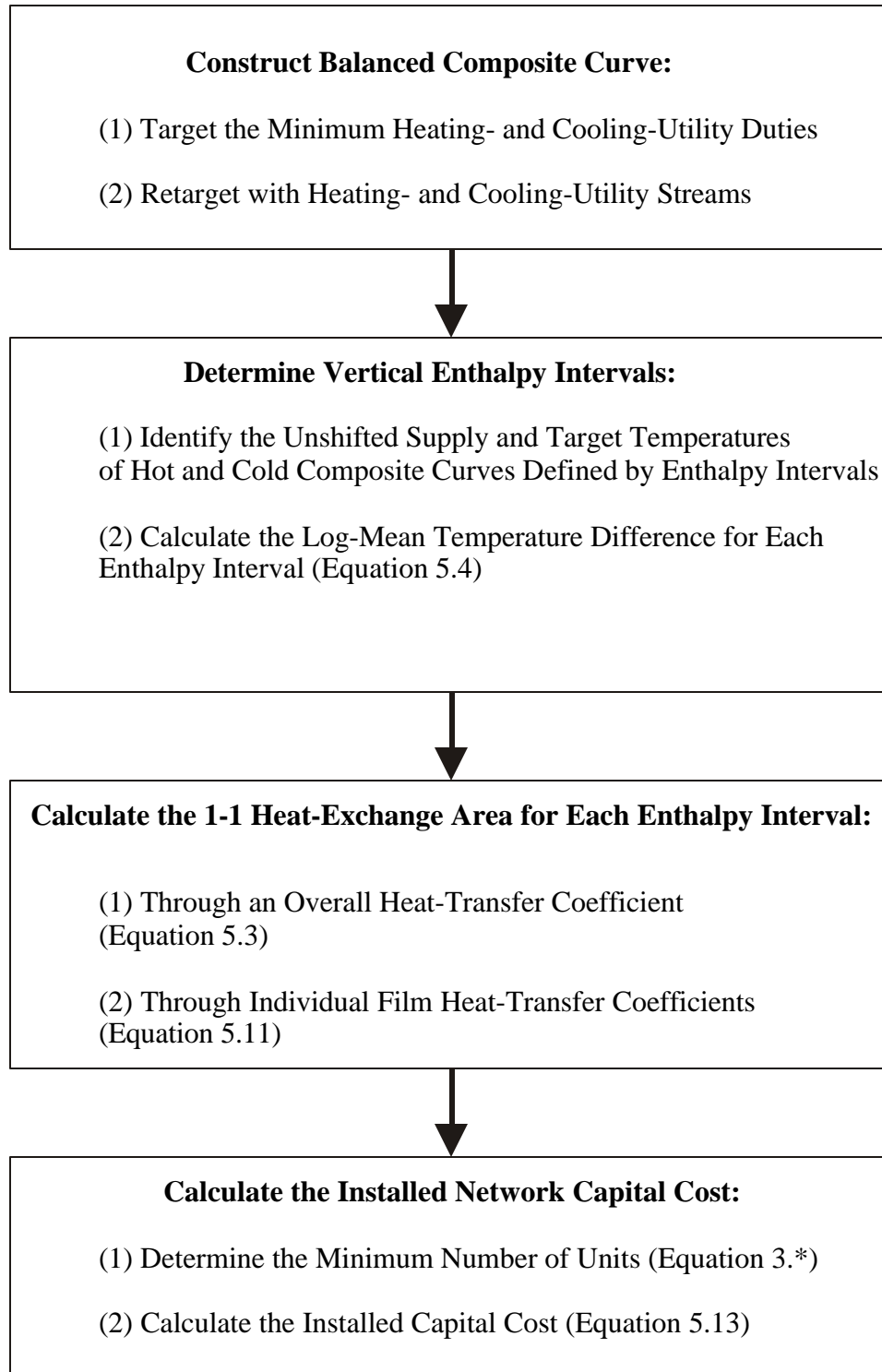


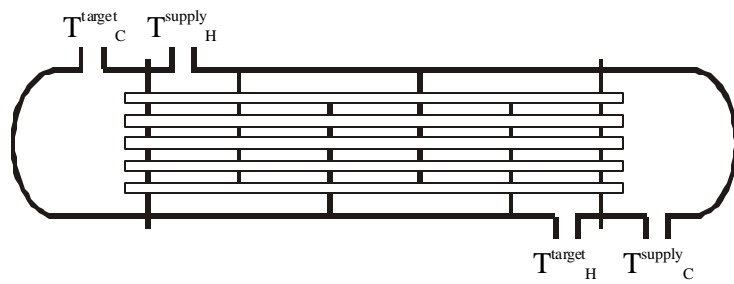
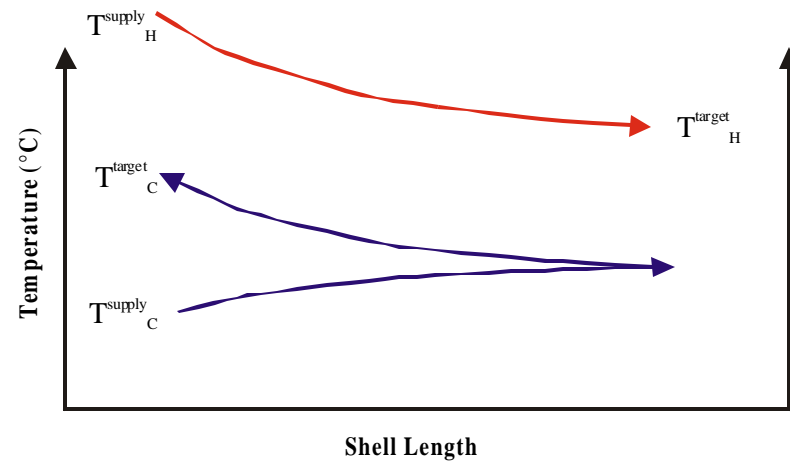
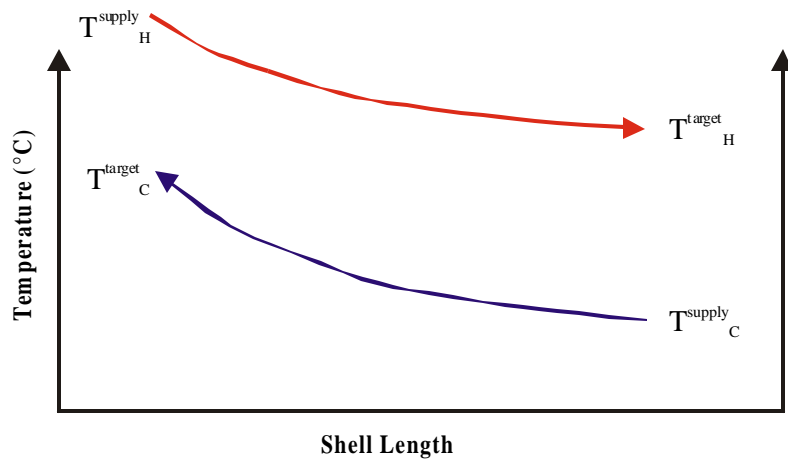
Figure 5.7. Illustration of the method for estimating the heat-exchange area and installed cost of a network of 1-1 exchangers.

5.3 Heat-Exchange Area and Capital Cost Targets for 1-2 Exchangers

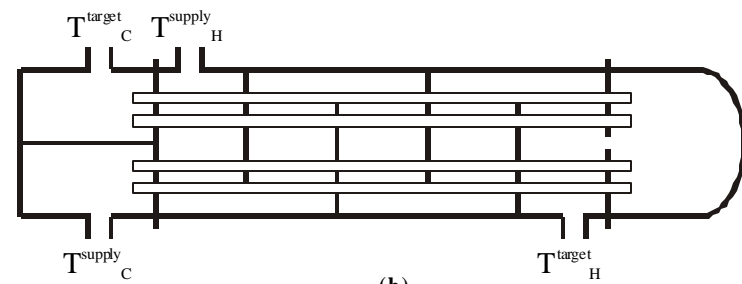
Figure 5.8 illustrates two common heat-exchanger configurations. Figure 5.8a shows a 1-shell-pass and 1-tube-pass (1-1) exchanger. Here, a temperature-enthalpy diagram exhibits countercurrent flow (i.e., the cold stream flows from right to left, and the hot stream flows from left to right). However, Figure 5.8b shows that in a 1-shell-pass and 2-tube-pass (1-2) exchanger, the shell- and tube-side fluids contact in first countercurrently and then cocurrently. The temperature-enthalpy diagram for the 1-2 exchanger shows that both hot and cold streams enter the unit to the left of the diagram. In this case, the cold stream flows first from left to right (cocurrent flow), then from right to left (countercurrent flow).

In most situations, the 1-1 exchanger is more effective in terms of heat-transfer area. In other words, the 1-1 exchanger typically requires a lower heat-transfer area than a 1-2 exchanger. However, 1-2 exchangers are preferred over 1-1 exchangers in several situations (Smith, 1995):

- 1-2 exchangers are easier to mechanically maintain than 1-1 exchangers.
- Higher tube-side velocities can increase tube-side film heat-transfer coefficients.
- Due to their configuration, 1-2 exchangers are better able to deal with thermal expansions.



(a)



(b)

Figure 5.8. Temperature profiles for two heat-exchanger configurations: (a) 1-shell-pass and 1-tube-pass (1-1) exchanger and (b) 1-shell-pass and 2-tube-pass (1-2) exchanger.

5.3.1 Area Target for a Network of Single 1-2 Exchangers

Equation 5.14 is the key design equation for 1-1 exchangers that approach countercurrent flow:

$$Q = UA\Delta T_{LM} \quad (5.14)$$

We correct Equation 5.14 for inefficient or non-countercurrent flow patterns (like that found in the 1-2 exchanger) by adding a LMTD (log –mean temperature difference) correction factor, F_T :

$$Q = UA\Delta T_{LM} F_T \quad (5.15)$$

where $0 < F_T < 1$.

Figure 5.9 is a graphical correlation of F_T for 1-2 exchangers through two dimensionless numbers, namely, the capacity ration R and the thermal efficiency P :

$$R = \frac{(\dot{M}C_p)_C}{(\dot{M}C_p)_H} = \frac{T_H^{\text{supply}} - T_H^{\text{target}}}{T_C^{\text{target}} - T_C^{\text{supply}}} \quad (5.16)$$

$$P = \frac{T_C^{\text{target}} - T_C^{\text{supply}}}{T_H^{\text{supply}} - T_C^{\text{supply}}} \quad (5.17)$$

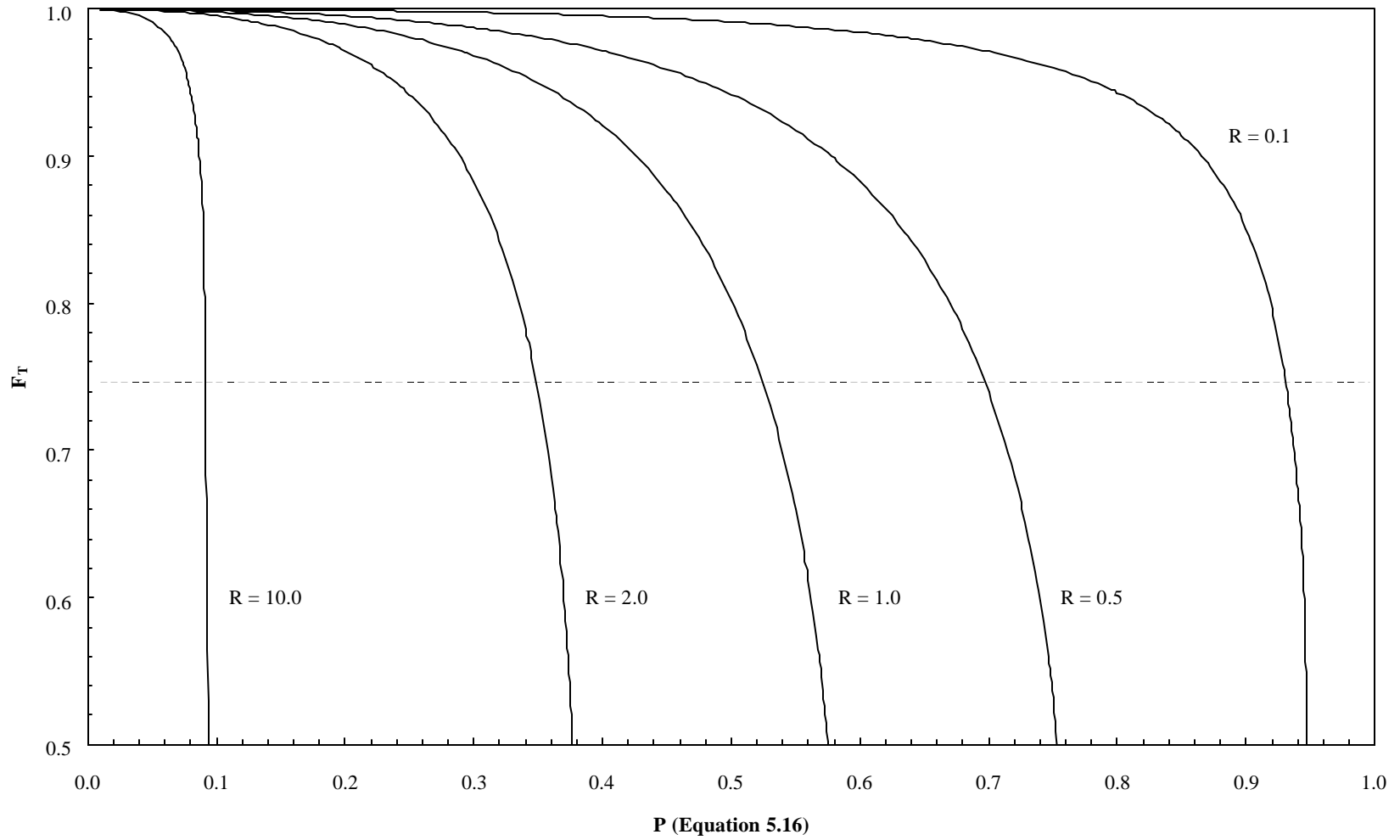


Figure 5.9. F_T correlation for 1-2 exchangers. The dimensionless numbers R and P are determined through Equations 5.15 and 5.16 for single 1-2 exchangers.

Equations 5.16 and 5.17 imply that F_T is only a function of the unshifted supply and target temperatures of hot and cold streams within an exchanger.

We modify Equation 5.12 to give the total heat-exchange area for a network of 1-2 exchangers by incorporating the correction factor, F_T :

$$A_{\text{network}} = \sum_k \left[\frac{1}{\Delta T_{\text{LM},k} F_{T,k}} \left(\sum_i \frac{q_{\text{Hi}}}{h_{\text{Hi}}} + \sum_j \frac{q_{\text{Cj}}}{h_{\text{Cj}}} \right) \right] \quad (5.18)$$

where the LMTD correction factor, F_T , is calculated from the unshifted supply and target temperatures of hot and cold composite curves as defined by enthalpy interval k via the dimensionless numbers R (Equation 5.16) and P (Equation 5.17).

Bowman, et al. (1940) gave a mathematical relationship for determining the LMTD correction factor with each enthalpy interval. When $R \neq 1$:

$$F_T = \frac{\sqrt{R^2 + 1} \ln \left[\frac{(1-P)}{(1-RP)} \right]}{(R-1) \ln \left\{ \frac{\left[2 - P \left(R + 1 - \sqrt{R^2 + 1} \right) \right]}{\left[2 - P \left(R + 1 + \sqrt{R^2 + 1} \right) \right]} \right\}} \quad (5.19)$$

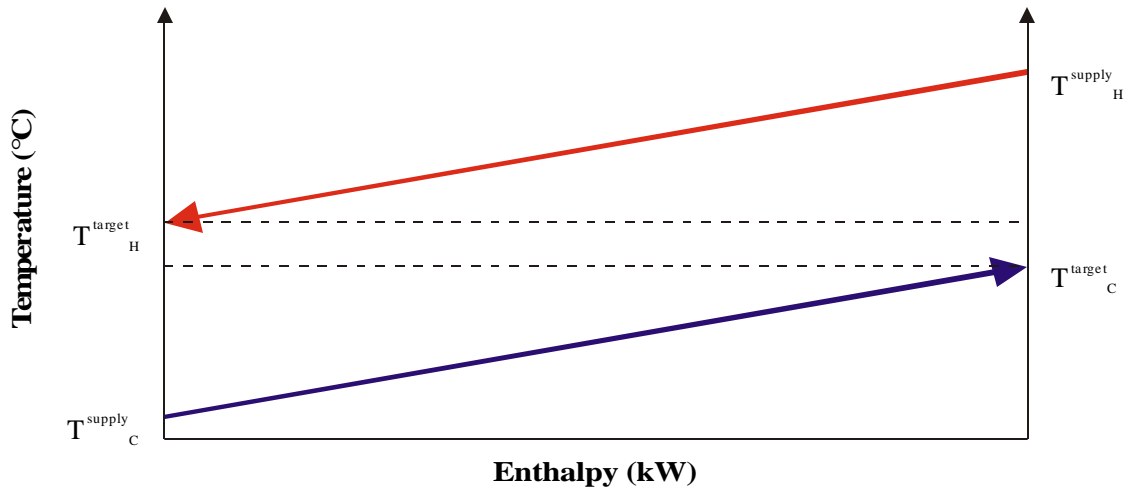
and when $R = 1$:

$$F_T = \frac{\left[\frac{\sqrt{2P}}{(1-P)} \right]}{\ln \left\{ \frac{2 - P(2 - \sqrt{2})}{2 - P(2 + \sqrt{2})} \right\}} \quad (5.20)$$

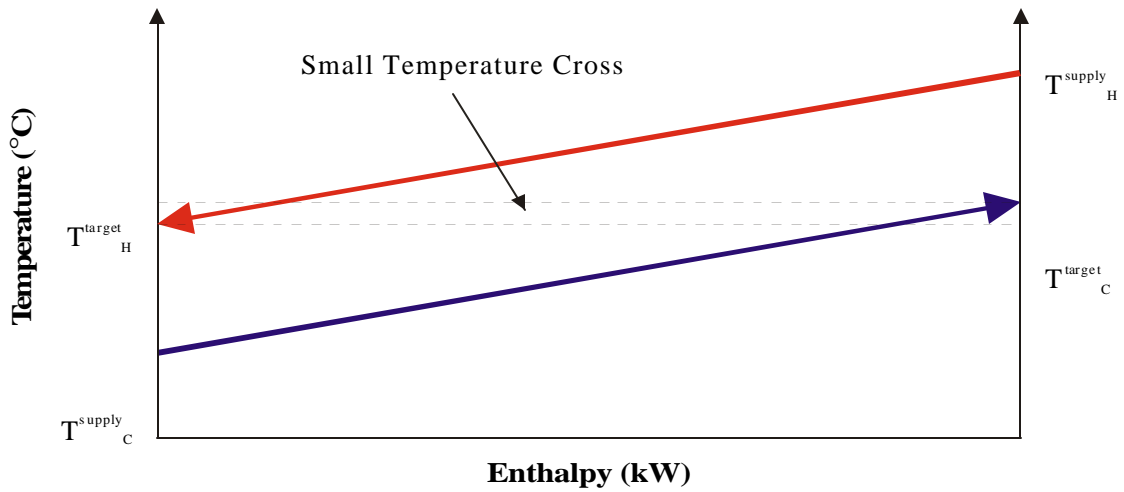
In many cases, heat transfer in 1-2 exchangers may not be feasible due to local reversals in heat-transfer driving force. The solution to this problem is to combine 1-2 shells in series. The following sections detail a general targeting procedure for the number of shells in series, total 1-2 heat-exchange area and installed capital costs for systems of 1-2 exchangers.

5.3.2 Area Target for a Network with 1-2 Shells in Series

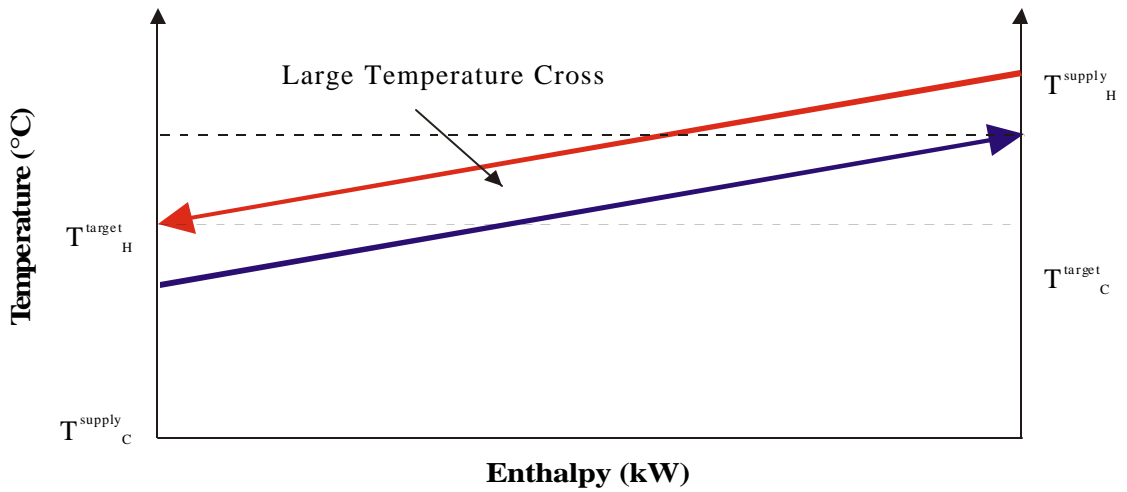
Figure 5.10 depicts the effect of the supply and target temperatures of hot and cold streams on the efficiency of a 1-2 exchanger (Ahmad, et al., 1988). In particular, we illustrate *the temperature cross* phenomenon. All three examples are feasible for true countercurrent flow (i.e., in a 1-1 exchanger). In fact, the example described by Figure 5.10a shows a large temperature-driving force throughout the exchanger.



(a)



(b)

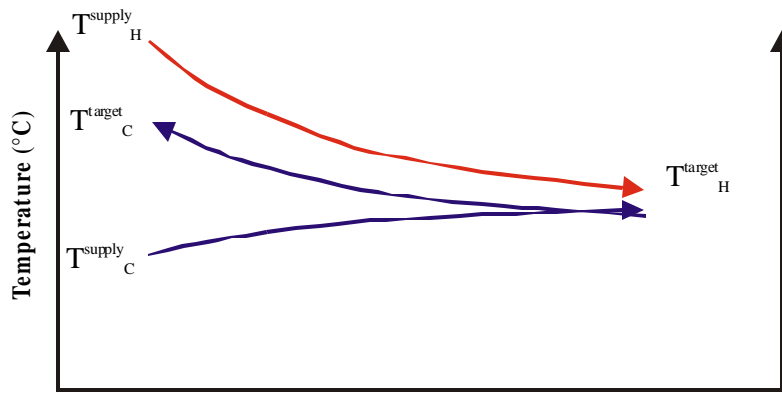


(c)

Figure 5.10. Temperature-enthalpy diagrams for three new examples in 1-1 exchangers. Examples (b) and (c) show temperature crosses between the target temperatures of hot and cold streams.

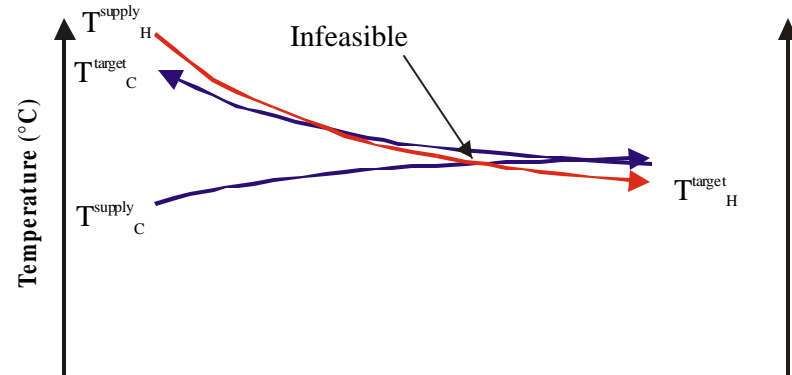
However, in both Figures 5.10b and c, we see temperature crosses. A temperature cross occurs when the cold-stream target temperatures lies above the hot-stream target temperature for true countercurrent flow. In the case of Figure 5.10b, the situation may still be feasible in a 1-2 exchanger. Specifically, Figures 5.11a and b illustrate temperature-enthalpy diagrams for 1-2 exchangers for the examples first shown in Figures 5.10b and c, respectively, for 1-1 exchangers. In Figure 5.11a, the effectiveness of the unit is reduced as a result of cocurrent flows to yield an approximate value for F_T equal of 0.75 for a 1-2 exchanger. Turning to the example shown in Figures 5.10c and 5.11b, we see a more severe temperature cross. The result is infeasible heat transfer within the 1-2 exchanger depicted by the heat-exchanger temperature profile shown in Figure 5.11b. In Figure 5.9, the F_T correlation for 1-2 exchangers shows the exchanger is operating well into the steep (unstable) portion of the R lines giving a LMTD correction factor, F_T well below the limit of 0.75.

A typical design procedure involves iteratively evaluating F_T for several different shell and tube combinations. The next logical step is to evaluate F_T for the example shown in Figures 5.10c and 5.11b in a 2 shell pass and 4 tube pass (2-4) exchanger. Figure 5.12 shows the temperature profile for this example in a 2-4 exchanger. This configuration appears feasible and we would expect a reasonable value (>0.75) for the correction factor F_T .



Shell Length

(a)



Shell Length

(b)

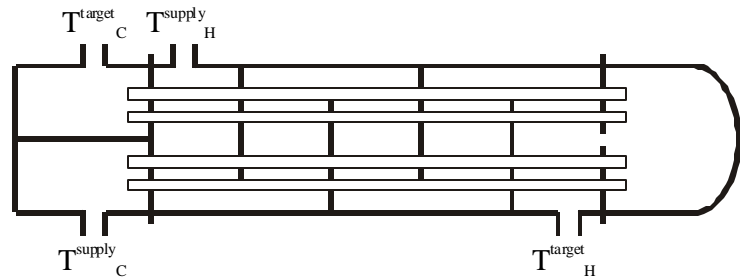


Figure 5.11. Temperature profiles for two examples first shown in Figures 5.10b and c in 1-2 exchangers. The 1-2 exchanger depicted by Figure 5.11b is infeasible

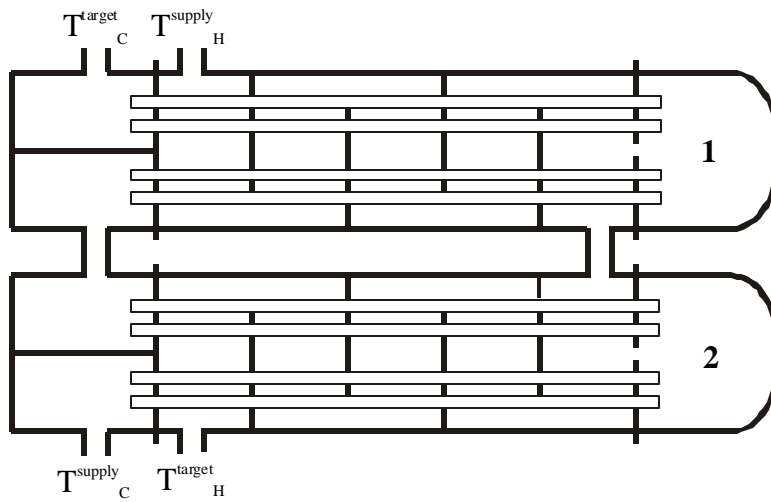
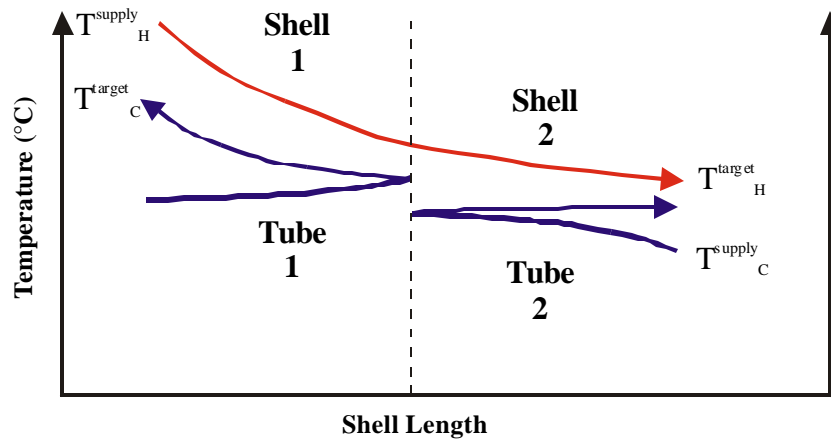


Figure 5.12. Temperature profile for the example shown in Figures 5.10c and 5.11b in a 2-shell-pass and 4-tube-pass (2-4) exchanger.

We must predict the number of shells when estimating the heat-exchange area and the capital cost of a heat-exchanger network consisting of more complex units (i.e., 1-2 and 2-4 exchangers). The trial-and-error method for evaluating the LMTD correction factor, F_T , of several exchanger configurations is not practical for our purposes. Instead, we rely on methods that predict the number of shells for a set of unshifted supply and target temperatures for hot and cold streams and a new factor X_P :

$$P = X_P P_{\max} \quad (5.21)$$

where X_P is chosen based on the asymptotic behavior of P with respect to F_T and R in Figure 5.9. In the figure, for any given value of R , P approaches an asymptotic limit as the LMTD correction factor F_T goes to zero. In other words, we select X_P such that F_T will remain above 0.75 and in a stable region of the R curve (i.e., we choose X_P so that F_T lies in a relatively flat portion of the R curve). A value of $X_P = 0.9$ usually insures F_T will remain above 0.75. Ahmad et al. Suggest that the maximum value of the dimensionless number P is:

$$P_{\max} = \frac{2}{R + 1 + \sqrt{R^2 + 1}} \quad (5.22)$$

The factor X_P allows us to identify the number of shells for a single unit based on the unshifted supply and target temperatures of hot and cold streams through dimensionless parameters R (Equation 5.16) and P (Equation 5.17). Note that, from this point forward, we denote the dimensionless number P as either P_{1-2} or P_{N-2N} where the subscript $N-2N$ reflects the number of shells (i.e., N is the number of 1-2 exchangers in series). When $R \neq 1$:

$$N_{\text{shells}} = \frac{\ln\left(\frac{1 - RP_{N-2N}}{1 - P_{N-2N}}\right)}{\ln W} \quad (5.23)$$

where W is defined as:

$$W = \frac{R + 1 + \sqrt{R^2 + 1} - 2RX_p}{R + 1 + \sqrt{R^2 + 1} - 2X_p} \quad (5.24)$$

When $R = 1$, we use:

$$N_{\text{shells}} = \frac{\left(\frac{P_{N-2N}}{1 - P_{N-2N}}\right) \left(1 + \frac{\sqrt{2}}{2} - X_p\right)}{X_p} \quad (5.25)$$

Here, we calculate R and P_{N-2N} through Equations 5.16 and 5.17, respectively, from the unshifted supply and target temperatures of hot and cold streams.

In practice, we use an integer number of shells. We denote the next higher integer number of 1-2 shells for a unit as $[N_{\text{shells}}]$. In general, we will use brackets to denote the next higher, integer number of shells.

Ahmad and Smith (1989) shows that the total number of shells for enthalpy interval k is related to the number of shells for a single unit, N_k , with unshifted supply and target temperatures for hot and cold composite curves defined by enthalpy interval k calculated through Equations 5.23 and 5.24 or Equation 5.26:

$$N_{\text{shells}_k} = N_k (S_k - 1) \quad (5.26)$$

where S_k is the total number of process and utility streams in enthalpy interval k .

Recall that we determine a value for $F_{T,k}$ either graphically or analytically (Equation 5.19 or 5.20). We can find $F_{T,k}$ through charts correlating F_T with the dimensionless numbers R (Equation 5.16) and P_{1-2} for a specific exchanger configuration (i.e., 1-2 versus 2-4 exchangers), or by calculating its value through Equation 5.19 or 5.20 for 1-2 exchangers. We use Equation 5.27 to find the dimensionless number P_{1-2} for more complex configurations (i.e., 2-4 and 3-6 exchangers) as a function of P_{N-2N} (Equation 5.17) and apply Equations 5.19 or 5.20 (Bowman, et al., 1940) to evaluate F_T :

$$P_{1-2} = \frac{1 - \left(\frac{1 - P_{N-2N} R}{1 - P_{N-2N}} \right)^{1/[N_k]}}{R - \left(\frac{1 - P_{N-2N} R}{1 - P_{N-2N}} \right)^{1/[N_k]}} \quad (5.27)$$

where $[N_k]$ is the next highest integer number of shells for a single unit with supply and target temperatures of hot and cold composite curves defined by the enthalpy interval k (i.e., the next highest integer number of shells from Equations 5.23 and 5.24 or 5.25).

Returning to Example 2.1, Table 5.8 lists the unshifted supply and target temperatures of hot and cold composite curves as well as the log-mean temperature difference defined by the vertical enthalpy intervals. The table includes the values of R_k (Equation 5.16), $P_{N-2N,k}$ (Equation 5.17), N_k (Equations 5.23 and 5.24 or 5.25), $[N_k]$, and P_{1-2} (Equation 5.27) that give a LMTD correction factor, F_T (Equation 5.19 or 5.20), in each vertical enthalpy interval k . The last column gives the 1-2 heat-exchange area for each interval. We easily determine the 1-2 heat-exchange area as:

$$A_{1-2,k} = \frac{A_{1-1,k}}{F_{T,k}} \quad (5.28)$$

Table 5.8. Data for determining the total 1-2 heat-transfer area for Example 2.1. Actual (unshifted) temperatures shown.

Enthalpy Interval k	Streams Present	$T^{\text{supply}}_{\text{HCC},k}$ (°C)	$T^{\text{target}}_{\text{HCC},k}$ (°C)	$T^{\text{supply}}_{\text{CCC},k}$ (°C)	$T^{\text{target}}_{\text{CCC},k}$ (°C)	$DT_{\text{lm},k}$ (°C)	R_k
1	H1,C3	75.00	55.00	20.00	22.91	42.98	6.875
2	H1,H2,C3	91.25	75.00	22.91	30.00	56.55	2.292
3	H1,H2,C1	101.25	91.25	50.00	70.00	36.02	0.500
4	H1,H2,C1,C2	135.00	101.25	70.00	115.00	25.21	0.750
5	H1,C1,C2	185.00	135.00	115.00	137.22	31.90	2.250
6	H3,C1,C2	209.14	209.00	137.22	142.00	69.43	0.030
7	H3,C1	210.00	209.14	142.00	185.00	42.66	0.020
Total							

Enthalpy Interval k	P_{N-2N}	W_k	N_k	$[N_k]$	P_{1-2}	F_T	$A_{1-2,k}$ (m ²)
1	0.053	0.188	0.238	1	0.053	0.995	70.17
2	0.104	0.418	0.371	1	0.104	0.994	130.10
3	0.390	2.100	0.748	1	0.390	0.974	171.09
4	0.692	1.375	4.204	5	0.272	0.984	816.50
5	0.317	0.425	2.035	3	0.168	0.979	320.11
6	0.066	8.580	0.062	1	0.066	1.000	23.22
7	0.632	9.014	0.449	1	0.632	0.996	227.62
Total							1758.81

5.3.3 Predicting the Total Number of Shells and Capital Cost

To be consistent with the pinch concept, we determine the total number of shells above and below the pinch temperature separately. We calculate the total number of shells for the entire problem by simply summing over the enthalpy intervals above and below the pinch:

$$N_{\text{shells}} = \sum_k N_{\text{shells}k} \quad (5.29)$$

or in terms of Equation 5.26:

$$N_{\text{shells}} = \sum_k N_k (S_k - 1) \quad (5.30)$$

Factoring Equation 5.30 reveals that we can also be determined the total number of shells by first summing the number of shells for each process and utility stream over all enthalpy intervals where that stream exists:

$$N_{\text{shells}} = \sum_k N_k S_k - \sum_k S_k \quad (5.31)$$

Here, $\sum_k N_k S_k$ is a streamwise shell-contribution term and can be rewritten in terms of the shell contribution of each stream i summed over all enthalpy intervals, $\sum_i \sum_k^{i \text{ exists}} N_k$. The second term in Equation 5.31 is the sum of the individual shell contributions of a stream defined by the supply and target temperatures of hot and cold composite curves over all enthalpy intervals, $\sum_k S_k$.

Equation 5.31 becomes:

$$N_{\text{shells}} = \sum_i \sum_k^{i \text{ exists}} N_k - \sum_k S_k \quad (5.32)$$

We can increase the accuracy of predicting the number of shells by considering the number of shells per stream across all enthalpy intervals (Smith, 1995). We calculate the shell area for each stream i both above and below the pinch:

$$\sum_k^{\text{where } i \text{ exists}} N_k \geq 1 \quad (5.33)$$

When completing the first term in Equation 5.32, we round the result of Equation 5.33 to one shell for those streams that contribute less than a complete shell both above and below the pinch temperature.

As a final check, we should compare the average area per shell to the maximum allowable area per shell both above and below the pinch:

$$\frac{A_{1-2, \text{Above the Pinch}}}{[N_{\text{shells}}]_{\text{Above the Pinch}}} \leq A_{1-2, \text{max}} \quad (5.34)$$

$$\frac{A_{1-2, \text{Below the Pinch}}}{[N_{\text{shells}}]_{\text{Below the Pinch}}} \leq A_{1-2, \text{max}} \quad (5.35)$$

If needed (i.e., if Equations 5.34 and/or 5.35 are violated), we can increase the number of shells above or below the pinch so that the average area per shell is just less than the maximum according to Equations 5.36 and 5.37:

$$[N_{\text{shells}}]_{\text{Above the Pinch}} = \left[\frac{A_{1-2, \text{Above the Pinch}}}{A_{1-2, \text{max}}} \right] \quad (5.36)$$

$$[N_{\text{shells}}]_{\text{Below the Pinch}} = \left[\frac{A_{1-2, \text{Below the Pinch}}}{A_{1-2, \text{max}}} \right] \quad (5.37)$$

Returning to Example 2.1, Table 5.8 lists the value of N_k both above (enthalpy interval 5 to 7) and below (enthalpy intervals 1 to 4) the pinch temperature. Table 5.9 lists the individual shell contributions of all streams both above and below the pinch. According to Equation 5.33, we increase the contribution from each stream to one for those with a contribution less than one both above and below the pinch. The second term in Equation 5.32 is the sum of the N_k column from Table 5.8 (equal to 8.108). Equation 5.32 gives:

$$\begin{aligned} N_{\text{shells}} &= \sum_i \sum_k^{\text{i exists}} N_k - \sum_k S_k \\ &= (24.494 + 4.476) - 8.108 \\ &= 20.862 \end{aligned}$$

Table 5.9. Shell contributions of all streams both above and below the pinch for the first term in Equation 5.32.

Shell Contribution		
Stream	Above the Pinch	Below the Pinch
H1	6.239	1.357
H2	4.204	1.119
H3	<i>0.511 => 1.0</i>	0
C1	6.750	<i>0.748 => 1.0</i>
C2	6.301	0
C3	0	<i>0.609 => 1.0</i>
Total	24.494	4.476

Finally, for a network of 1-2 exchangers, we estimate the total installed capital cost by modifying Equation 5.13 to include the additional shells determined through Equations 5.32 through 5.37:

$$\text{Capital Cost} = N_{\text{shells}} \left[a + b \left(\frac{A_{1-2,\text{network}}}{N_{\text{shells}}} \right)^c \right] \quad (5.38)$$

where $A_{1-2,\text{network}}$ is the total network area for 1-2 exchangers and N_{shells} is the total number of shells determined through Equations 5.32 through 5.37 above and below the pinch.

For Example 2.1, we use the heat-exchanger cost coefficients for a network of carbon-steel exchangers (Table 5.4) in Equation 5.38 to generate an estimated installed cost for a network of 1-2 exchangers equal to \$1,744,000.

$$\begin{aligned}
 \text{Capital Cost} &= N_{\text{shells}} \left[a + b \left(\frac{A_{1-2,\text{network}}}{N_{\text{shells}}} \right)^c \right] \\
 &= 21 \left[0 + (\$3,000/\text{m}^{1.5}) \left(\frac{1758.81 \text{ m}^2}{21} \right)^{0.75} \right] \\
 &= \$1,744,000
 \end{aligned}$$

Equation 5.3 gives the annualized total cost without interest:

$$\begin{aligned}
 (\text{Total Annualized Cost}) &= (\text{Operation Cost}) + \frac{(\text{Capital Cost})}{t} \\
 &= \$1,314,000/\text{yr} + \frac{\$1,744,000}{5 \text{ yr}} \\
 &= \$1,663,000/\text{yr}
 \end{aligned}$$

Figure 5.13 summarizes this method for estimating the heat-exchange area and installed cost for a network of 1-2 exchangers.

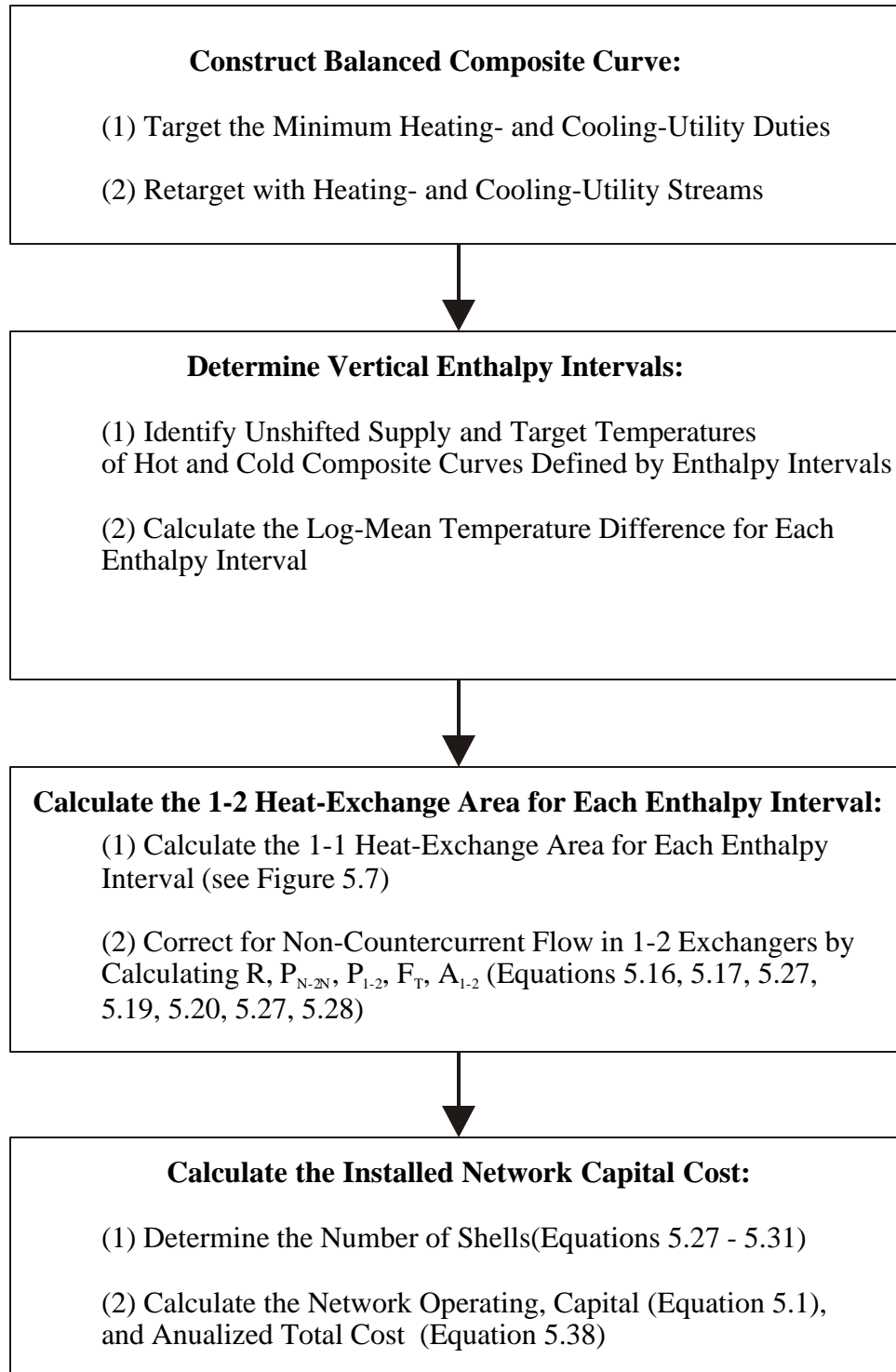


Figure 5.13. Illustration of the method for estimating the heat-exchange area and installed cost for a network of 1-2 exchangers.

5.4 SuperTargeting: Optimizing the Minimum Approach Temperature

To this point, we have chosen a value for the minimum approach temperature, ΔT_{\min} , based on past experiences. Now, through the techniques described in the previous sections, we can predict the heat-exchange area and the total annualized cost of a network prior to any detailed design and optimize our network by selecting a value for the MAT that minimizes the annualized cost of the network.

By varying the minimum approach temperature, we determine values for the utility consumption and cost, heat-exchange area and capital cost, and finally the annualized total cost. These calculations are tedious and most often performed through commercial software tools. Data for Figures 5.14 to 5.16 were generated through the commercial software tool Aspen Pinch. Figure 5.14 shows that a MAT of 8 to 10 °C minimizes total cost. Figure 5.15 displays the heating- and cooling-utility duties as a function of the MAT and Figure 5.16 depicts the number of shells target versus the MAT.

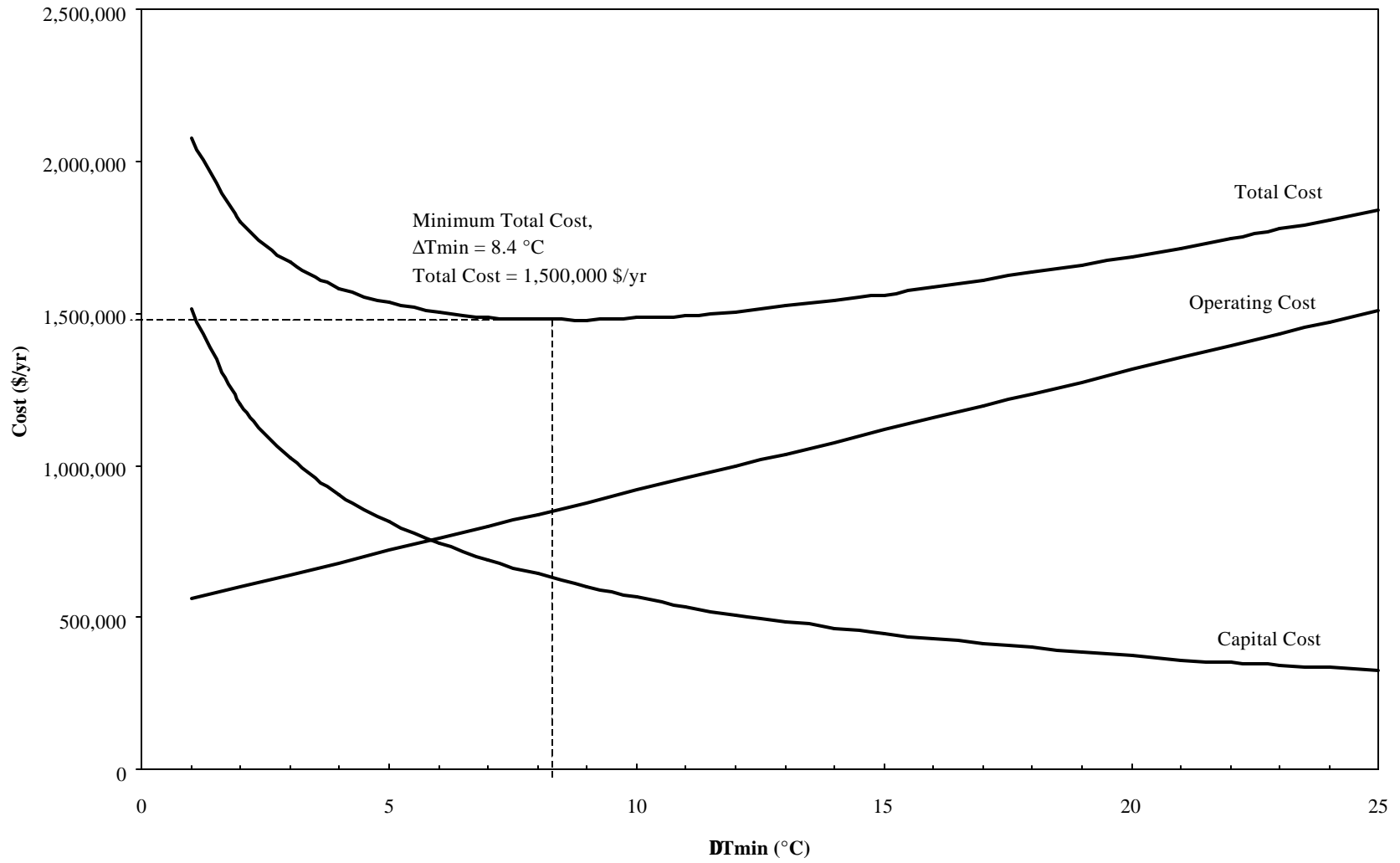


Figure 5.14. Optimizing the minimum approach temperature based on operating, capital and total costs for Example 2.1 through Aspen Pinch .

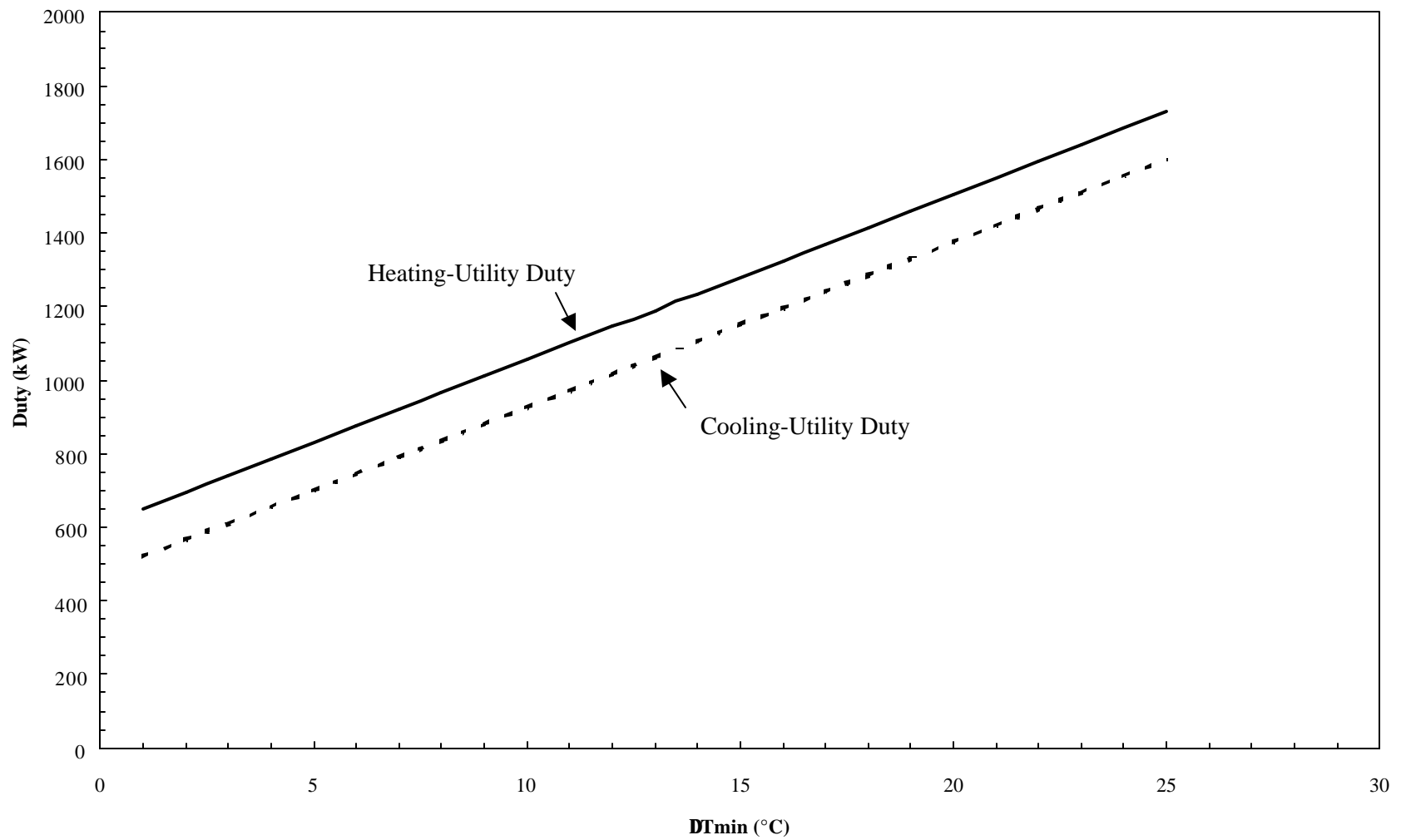


Figure 5.15. Heating- and cooling-utility consumption versus the minimum approach temperature for Example 2.1 through *Aspen Pinch*.

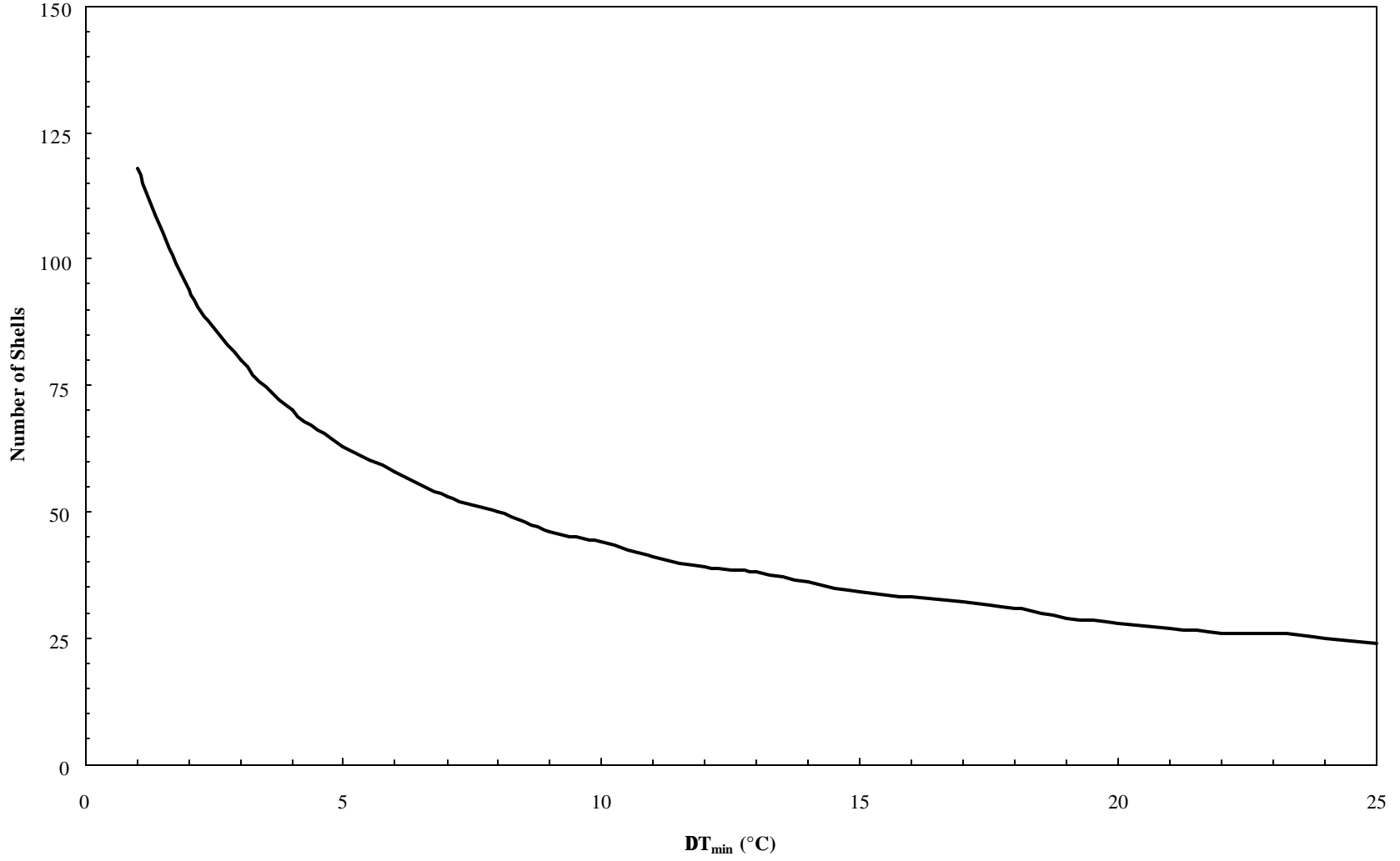


Figure 5.16. Number of shells for Example 2.1 versus the minimum approach temperature through *Aspen Pinch*.

5.5 Summary

- Previous chapters did not consider the economic feasibility of maximum-energy-recovery (MER) networks. We introduce methods for evaluating operating costs, heat-exchange area, capital cost and total cost for heat-exchanger networks. This allows us to evaluate alternative flowsheets and utility systems to balance operating and capital costs.
- We modify hot and cold composite curves to include heating and cooling utilities making the minimum heating- and cooling-utility duties, identified on the balanced composite curve zero.
- Operating costs include heating- and cooling-utility costs.
- We present techniques for estimating the heat-exchange area for networks of one-shell-pass and one-tube-pass (1-1) exchangers (Section 5.2) and one-shell-pass and two-tube-pass (1-2) exchangers (Section 5.3).
- Capital costs include heat-exchanger equipment. We use correlations to calculate capital costs of heat-exchanger networks from heat-exchange area, minimum number of shells and the configuration and materials of construction of the exchangers.

- Commercial software tools automate the methods presented in this chapter for evaluating the heat-exchange area, capital cost and total cost of a heat-exchanger networks and optimizing these networks with respect to the minimum approach temperature.

Nomenclature

$A_{1-1,k}$	1-1 Heat exchange area for enthalpy interval k, m ²
$A_{1-1, \text{network}}$	1-1 Heat exchange area for a heat-exchanger network, m ²
$A_{1-2,k}$	1-2 Heat exchange area for enthalpy interval k, m ²
$A_{1-2, \text{max}}$	Maximum 1-2 Heat exchange area for a single unit, m ²
ΔH_k	Enthalpy change in enthalpy interval k, kW
$\Delta T_{LM,k}$	Log-mean temperature difference for enthalpy interval k, °C
ΔT_{min}	Minimum approach temperature, °C
$F_{T,k}$	LMTD correction factor for enthalpy interval k, dimensionless
h_{Cj}	Film-heat-transfer coefficient for cold stream j, kW/(m ² · °C)
h_{Hi}	Film-heat-transfer coefficient for hot stream i, kW/(m ² · °C)
$(\dot{M}C_p)_i$	Capacity flowrate of process stream i, kW/°C
N_C	Number of cold process streams
N_{CU}	Number of cold utilities
N_H	Number of hot process streams
N_{HU}	Number of hot utilities
N_k	Number of 1-2 heat-exchanger shells for a single unit
$[N_k]$	Next higher integer number of number of 1-2 heat-exchanger shells for a single unit
N_{shells}	Number of 1-2 heat-exchanger shells for a heat-exchanger network

$N_{\text{shells},k}$	Number of 1-2 heat-exchanger shells for a heat-exchanger network in enthalpy interval k
$[N_{\text{shells}}]$	Next higher integer number of 1-2 heat-exchanger shells
N_{units}	Minimum number of units
P	Capacity ratio, dimensionless
P_{1-2}	Capacity ratio for 1-2 exchangers, dimensionless
P_{N-2N}	Capacity ration for 1-2 exchangers, dimensionless
P_{max}	Asymptotic limit for the capacity ratio, dimensionless
$Q_{\text{Hi},\text{Cj}}$	Heat load of a match between hot stream i and cold stream j, kW
q_{Cj}	Enthalpy change of cold stream j in enthalpy interval k, kW
q_{Hi}	Enthalpy change of hot stream i in enthalpy interval k, kW
R	Thermal efficiency, dimensionless
$T_{\text{CCC},k}^{\text{supply}}$	Unshifted supply temperature of the cold composite curve defined by enthalpy interval k, °C
$T_{\text{HCC},k}^{\text{supply}}$	Unshifted supply temperature of the hot composite curve defined by enthalpy interval k, °C
$T_{\text{CCC},k}^{\text{target}}$	Unshifted target temperature of the cold composite curve defined by enthalpy interval k, °C
$T_{\text{HCC},k}^{\text{target}}$	Unshifted target temperature of the hot composite curve defined by enthalpy interval k, °C
U	Overall heat-transfer coefficient, kW/(m ² · °C)
$U_{\text{Hi},\text{Cj}}$	Overall heat-transfer coefficient a match between hot stream i and cold stream j, kW/(m ² · °C)

X_p

Capacity ratio limiting factor, dimensionless

References

Ahmad, S., Linnhoff, B. and Smith, R., "Cost Optimum Heat Exchanger Networks: II. Targets and Design for Detailed Capital Cost Models," *Computers Chem. Eng.*, 10: 591 (1986).

Ahmad, S., Linnhoff, B. and Smith, R., "Design of Multipass Heat Exchangers: An Alternative Approach," *Trans. ASME, J. Heat Transfer*, 110: 304 (1988).

Ahmad, S. and Smith, R., "Targets and Design for Minimum Number of Shells in Heat Exchanger Networks," *ICHEME, ChERD*, 67: 481 (1989).

Bowman, R. A., Mueller, A. C. and Nagle, W. M., "Mean Temperature Differences in Design," *Trans. ASME*, 62: 283 (1940).

Linnhoff, B., Townsend, D. W., Boland, D., et al., "A User Guide to Process Integration for the Efficient Use of Energy," *ICHEME UK* (1982).

Shenoy, U. V., *Heat Exchanger Network Synthesis: Process Optimization by Energy and Resource Analysis*, Gulf Publishing Company, Houston (1995).

Smith, R., *Chemical Process Design*, McGraw-Hill, New York (1995).

Townsend, D. W., and Linnhoff, B., "Surface Area Targets for Heat Exchanger Networks,"
IChemE Annual Research Meeting, Bath, U.K. (1984).